Brief sensory deprivation triggers plasticity of neurotransmitter-synthesising enzyme expression in genetically labelled olfactory bulb dopaminergic neurons

Darren J Byrne, Marcela Lipovsek, Matthew S Grubb

Centre for Developmental Neurobiology, Institute of Psychiatry, Psychology and Neuroscience (IoPPN), King's College London, UK

Correspondence: matthew.grubb@kcl.ac.uk

Abstract

In the glomerular layer of the olfactory bulb, local dopaminergic interneurons play a key role in regulating the flow of sensory information from nose to cortex. These dual dopamine- and GABA-releasing cells are capable of marked experience-dependent changes in the expression of neurotransmitter-synthesising enzymes, including tyrosine hydroxylase (TH). However, such plasticity has most commonly been studied in cell populations identified by their expression of the enzyme being studied, and after long periods of sensory deprivation. Here, instead, we used brief 1- or 3-day manipulations of olfactory experience in juvenile mice, coupled with a conditional genetic approach that labelled neurons contingent upon their expression of the dopamine transporter (DAT-tdTomato). This enabled us to evaluate the potential for faster changes in neurotransmitter-synthesising enzyme expression in an independently identified population of neurons. Our labelling strategy showed good specificity for olfactory bulb dopaminergic neurons, whilst also revealing a minority sub-population of non-dopaminergic DAT-tdTomato cells that expressed the calcium-binding protein calretinin. Crucially, the proportions of these neuronal subtypes were not affected by brief alterations in sensory experience. Short-term olfactory manipulations also produced no significant changes in immunofluorescence for the GABA-synthesising enzyme GAD67. However, in bulbar DAT-tdTomato neurons brief sensory deprivation was accompanied by a transient drop in immunofluorescence for the dopamine-synthesising enzyme dopa decarboxylase (DDC), and a sustained decrease in TH expression. Careful characterisation of an independently identified, genetically labelled neuronal population therefore enabled us to uncover experience-dependent changes in neurotransmitter-synthesising enzyme expression that are more rapid than previously appreciated.

32 **Introduction**

33

34 Dopaminergic neurons in the mammalian olfactory bulb form a neurochemically-distinct population
35 of glomerular layer interneurons (Hökfelt *et al.*, 1975; Kosaka & Kosaka, 2007, 2011). They are dual-
36 transmitter cells, releasing both dopamine and GABA to locally modulate information being sent
37 from nose to cortex (Borisovska *et al.*, 2013; Liu *et al.*, 2013, 2016; Banerjee *et al.*, 2015; Pignatelli &
38 Belluzzi, 2017; Vaaga *et al.*, 2017). Production of these transmitters is undertaken by specialised
39 enzymatic pathways, which include tyrosine hydroxylase (TH) as the rate-limiting step in dopamine
40 synthesis, and DOPA decarboxylase (DDC) as its immediate downstream partner (Halász *et al.*, 1977).
41 Glutamate decarboxylase (GAD)-67, on the other hand, is the GABA-synthesising enzyme that is
42 ubiquitously expressed in this neuronal class (Kiyokage *et al.*, 2010; Kosaka *et al.*, 2019).

43 Expression levels of these neurotransmitter-synthesising enzymes are a well characterised target of
44 activity-dependent plasticity in olfactory bulb dopaminergic neurons. TH, especially, is exquisitely
45 sensitive to changes in sensory input. Since the landmark descriptions of decreased TH enzymatic
46 activity and immunofluorescence in the bulb following damage to the peripheral olfactory system
47 (Nadi *et al.*, 1981; Baker *et al.*, 1983), a wealth of evidence has shown that both *Th* mRNA and TH
48 protein levels in bulbar cells track alterations in olfactory sensory neuron activity (Baker *et al.*, 1984,
49 1993, 1999; Kosaka *et al.*, 1987; Baker, 1990; Stone *et al.*, 1990; Cho *et al.*, 1996; Philpot *et al.*, 1998;
50 Saino-Saito *et al.*, 2004; Bastien-Dionne *et al.*, 2010; Cave *et al.*, 2010; Weiss *et al.*, 2011; Grier *et al.*,
51 2016). Indeed, these TH changes are so reliable and sensitive that they are often used as
52 confirmation that particular olfactory system manipulations have been effective (Wilson & Sullivan,
53 1995; Mandairon *et al.*, 2006; Kass *et al.*, 2013). Olfactory bulb GAD67 has received rather less
54 attention, but nevertheless has also been shown to undergo experience-dependent changes in both
55 mRNA (*Gad1*) and protein levels (Parrish-Aungst *et al.*, 2011; Lau & Murthy, 2012; Banerjee *et al.*,
56 2013; Wang *et al.*, 2017).

57 The vast majority of these activity-dependent enzyme expression changes have been detected
58 following relatively prolonged manipulations of sensory input, usually on the order of weeks.
59 However, there are indications that transmitter-synthesising enzyme expression can change more
60 rapidly. A significant decrease in whole-bulb *Th* mRNA has been observed after only 2 d of unilateral
61 naris occlusion (Cho *et al.*, 1996). *In vitro*, increases in TH immunofluorescence or TH-GFP transgene
62 levels have been observed after just 24 h of sustained depolarisation in dissociated and slice
63 cultures, respectively (Akiba *et al.*, 2007; Chand *et al.*, 2015). We also recently found that a 24 h
64 period of *in vivo* sensory deprivation was associated with a decrease in relative immunofluorescence

65 in olfactory bulb TH-positive neurons, without any accompanying change in their density within the
66 glomerular layer (Galliano *et al.*, 2020).

67 A significant caveat is that, to date, these changes in neurotransmitter-synthesising enzyme
68 expression have all been detected either by employing tissue-level analyses that encompass the full
69 range of bulbar cell types, or by using the measured variable itself (e.g. TH immunofluorescence) to
70 identify individual cells to be studied. Ideally, gaining cell-type-specific information regarding
71 plasticity in enzyme expression would instead use an independent marker of cell identity. This
72 would enable experience-dependent changes to be identified amongst a consistently identified
73 group of neurons, without the potential distortion that can result when a plastic variable determines
74 which cells to measure. Here, we therefore took advantage of a conditional mouse transgenic line,
75 $DAT^{IRES\mathit{cre}}$ (Bäckman *et al.*, 2006), which when crossed with an appropriate reporter line generates
76 selective fluorescent label in cells that express the dopamine transporter (DAT-tdTomato). We
77 quantitatively characterised the selectivity of this line and found that it labels a small subset of
78 calretinin-expressing cells in addition to a majority of olfactory bulb dopaminergic neurons.
79 Crucially, this subtype specificity was unaffected by manipulations used to induce brief olfactory
80 deprivation. We found that such short-term, naturally relevant sensory manipulations do not affect
81 relative levels of GAD67 immunofluorescence in olfactory bulb DAT-tdTomato cells. In contrast,
82 deprivation does lead to transient and sustained decreases in the relative expression of DDC and TH,
83 respectively, within this independently identified population of neurons.

84 **Methods**

85

86 *Animals*

87 Mice of either gender were used and housed under a 12 h light:dark cycle in an environmentally
88 controlled room with access to water and food ad libitum. Day of birth was designated as P0.
89 DAT$^{IRES cre}$ mice (B6.SJL-*Slc6a3*$^{tm1.1(cre)Bkmn/J}$, Jax stock 006660; Bäckman *et al.*, 2006) were crossed with
90 Rosa26-floxed stop tdTomato reporter mice (Gt(ROSA)26Sor$^{tm9(CAG-tdTomato)Hze}$, Jax stock 007909) to
91 generate DAT-tdTomato mice. Wild type C57/Bl6 mice (Charles River) were used to back cross each
92 generation of transgenic mice. All experiments were performed at King's College London under the
93 auspices of UK Home Office personal and project licences held by the authors.

94

95 *Unilateral naris occlusion*

96 Olfactory sensory deprivation was induced by unilateral naris occlusion, using a custom made plug
97 (Cummings *et al.*, 1997). Each plug was constructed by knotting suture (Ethicon Ethilon
98 Monofilament Polyamide 6) around a piece of unscented dental floss pulled through the lumen of
99 PTFE tubing with an outer diameter of 0.6 mm and inner diameter of 0.3 mm (VWR International,
100 cat#: S1810 04). Mice were briefly anaesthetised with isoflurane and the plug trimmed, coated in
101 petroleum jelly and inserted into the right naris. Mice were returned to their home cage and left for
102 1 or 3 days before tissue collection. Presence of the nose plug was confirmed by examining the nasal
103 cavity after olfactory bulb dissection *ex vivo*. Sham controls, used for qPCR experiments only, had a
104 nose plug inserted into the right naris and immediately removed. Anaesthetised controls, used for all
105 other experiments, were handled and anaesthetised briefly with isoflurane but had no plug inserted
106 into either naris.

107

108 *Transcardial perfusion and histology*

109 P28 and P30 DAT-tdTomato mice were anaesthetised with an intraperitoneal overdose of
110 pentobarbital, then transcardially perfused with 20 mL phosphate buffered saline (PBS) with
111 20 U/mL heparin, followed by 20 mL of 4 % paraformaldehyde (PFA) in PIPES buffer (3 % sucrose,
112 60 mM PIPES, 25 mM HEPES, 5 mM EGTA, and 1 mM $MgCl_2$). PFA was prepared in batches, frozen at
113 -20 °C and defrosted shortly before use. On completion of perfusion, the mouse was decapitated,
114 and the brain removed from the skull and post-fixed in 4% PFA overnight. The brain was then

115 washed with PBS (3x5 minutes) and stored in PBS with 0.05% sodium azide for up to 6 months. For
116 sectioning, brains were embedded in 6% agarose and sliced coronally at 50 µm using a vibratome
117 (Leica VT1000s; Wetzlar, Germany). Slices were stored in PBS and 0.05% sodium azide at 4 °C before
118 staining.

119

120 *Immunohistochemistry*

121 Free-floating slices were incubated at room temperature (RT; 18-24 °C) for 2 hours in a blocking and
122 permeabilising solution (10% normal goat serum in PBS containing 0.25% Triton-X and 0.02% sodium
123 azide). They were then incubated in primary antibody diluted in the blocking solution at 4 °C for
124 between 18-24 hours (see Table 1 for antibodies used and their working dilution; endogenous
125 tdTomato fluorescence was always enhanced with immunolabel for red fluorescent protein). For
126 immunofluorescence intensity analysis, slices were incubated for approximately 72 hours in primary
127 antibody solution. Slices were then washed with PBS (3x5 minutes) and incubated in the species-
128 appropriate secondary antibody (Alexa Fluor® Life Technologies) diluted 1: 1,000 in the blocking
129 solution at RT for 2 hours. After 3x5 minutes washes in PBS, slices were mounted on glass slides with
130 MOWIOL® (Millipore).

131

Antigen	Host Species	Working Dilution	Supplier (product code)
Calbindin	Rabbit	1: 5,000	Swant (CB38a)
Calretinin	Mouse	1: 5,000	Millipore (MAB1568)
	Rabbit	1: 5,000	Swant (7699/3H)
cFos	Mouse	1: 1,000	Santa Cruz (sc166940)
Dopa decarboxylase (DDC)	Mouse	1: 1,000	Santa Cruz (sc-293287)
Glutamate decarboxylase 67 (Gad67)	Mouse	1: 500	Millipore (MAB351R)
Red fluorescent protein (tdTomato)	Rabbit	1: 1,000	Clontech (632496)
	Rat	1: 1,000	Chromotek (5F8)
Tyrosine hydroxylase (TH)	Mouse	1: 1,000	Millipore (MAB318)
	Rabbit	1: 1,000	Millipore (AB152)

132 **Table 1:** Details of primary antibodies

133

134 *Image acquisition and experimental design*

135 All images were acquired with a laser scanning confocal microscope (Zeiss LSM 710 Axio Examiner
136 Z1) using appropriate excitation and emission filters, a pinhole of 1 AU and a 40x oil immersion
137 objective. Laser power, gain and offset were manually set to prevent fluorescence saturation and
138 ensure optimum signal-to-noise.

139 For analyses of relative immunofluorescence intensity, we aimed to minimise and control for
140 between-section experimental variability. To reduce the effect of the homecage environment, each
141 experimental 'set' of four mice belonged to the same litter and was exposed to the same external
142 odour environment until unilateral naris occlusion or control procedure at P27. All mice were
143 returned to the homecage and left for 1 or 3 days. Perfusions and post-fixing were performed using
144 the same batch of PFA for each set, and mice within each set were perfused within 30 minutes of
145 each other. Brains from the same set were trimmed to the same size and co-embedded in 6%
146 agarose to ensure all brains would be sliced together. The agarose block was cut with landmarks to
147 ensure each mouse could be reliably identified. Co-embedded slices were processed for
148 immunohistochemistry as described above, with primary antibodies applied for 72 hours. Therefore,
149 all control and occluded sections on each slice were exposed to identical reagents at identical
150 concentrations for identical periods of time. The olfactory bulb sections in a co-embedded slice were
151 then imaged on the same day using identical laser and detection settings that were optimised for
152 that co-embedded slice. Z-stacks were taken from different parts of an olfactory bulb slice, setting
153 the start and end Z positions using the DAT-tdTomato fluorescence. Images were acquired at a
154 resolution of 512 x 512 pixels (0.277 µm /pixel) and a Z step of 1 µm.

155 Images for analysing colocalisation of DAT-tdTomato with other markers were acquired at a
156 resolution of 512 x 512 pixels (0.277 µm /pixel) and a Z step of 1 µm, with multiple Z stacks taken
157 around the entire olfactory bulb section.

158 All immunohistochemistry, imaging and image analysis of tissue from mice that had been
159 manipulated was performed blind to experimental group.

160

161 *Image analysis*

162 All image analysis was performed using ImageJ software (Fiji). Cells were counted manually using the
163 cell counter plugin and only if their soma was entirely inside the image area. Soma size and
164 fluorescence intensity were measured at the neuron's widest area in the Z-stack, identified when the
165 soma was larger than in the slice above and below. For measuring immunofluorescence intensity,

166 neurons were manually identified for analysis solely by the expression of DAT-tdTomato. TH and
167 GAD67 immunolabel were located primarily outside the nucleus, therefore, average
168 immunofluorescence intensity (mean grey value; MGV) was measured in the somatic cytoplasm
169 only, using a hand-drawn polygonal region of interest (ROI). For DDC and cFos, MGV was measured
170 across the entire soma, again using a hand-drawn polygonal ROI. All tdTomato cells that had the
171 entire cell body within the image area and for which the widest soma area could be confirmed were
172 measured in each stack.

173 For immunofluorescence intensity analysis, background MGV values were taken from unlabelled
174 bulbar regions of each Z-stack and were subtracted from the MGV of each cell in that Z-stack. MGV
175 values were then normalised to the control average (1 and 3 day) in each slice.

176

177 *Electrophysiology*

178 For acute slice preparation, mice were deeply anaesthetised with isoflurane and decapitated. The
179 olfactory bulb and frontal cortices were rapidly removed and transferred into ice-cold sucrose slicing
180 medium (containing in mM: 240 sucrose, 5 KCl, 1.25 Na_2HPO_4, 2 $MgSO_4$, 1 $CaCl_2$, 26 $NaHCO_3$ and 10
181 D-glucose, bubbled with 95% O_2 °and 5% CO_2). 300 µm horizontal sections of the olfactory bulb were
182 cut using a Leica vibratome (VT1000S) (Wetzlar, Germany) and were transferred to standard artificial
183 CSF (ACSF; containing in mM: 124 NaCl, 5 KCl, 1.25 Na_2HPO_4, 2 $MgSO_4$, 2 $CaCl_2$, 26 $NaHCO_3$ and 20 D-
184 glucose; with 10 µM NBQX, 50 µM APV, 10 µM SR-95531 to block major ionotropic synaptic
185 receptors, continuously bubbled with 95% O_2 and 5% CO_2, pH 7.4, ~310 mOsm). Slices were left to
186 recover at RT for at least 45 minutes before experiments began.

187 For whole-cell recordings, individual slices were secured in a chamber mounted on a Nikon FN1
188 microscope. DAT-tdTomato neurons were visualised with a 40x water immersion objective and
189 tdTomato fluorescence was revealed by under LED illumination (CoolLED pE-100) with appropriate
190 excitation and emission filters (ET575/50m, CAIRN Research, UK). Slices were continuously
191 superfused with ACSF heated to physiologically relevant temperature (34 ± 1 C) using an in-line
192 solution heater (TC-344B, Warner Instruments). Recordings were carried out using a Heka EPC10/2
193 amplifier coupled to PatchMaster acquisition software. Signals were digitised and sampled at 20 kHz.
194 Recording electrodes were pulled from borosilicate glass [outer diameter (OD), 1.5 mm; inner
195 diameter (ID), 1.17 mm] (GT100T-10, Harvard Apparatus) with a vertical puller (PC-10, Narishige) and
196 the tip fire-polished with a microforge (MF-830, Narishige). Pipettes with 3-5 MΩ resistance were
197 filled with K-gluconate-based intracellular solution, containing, in mM: 124 K-gluconate, 9 KCl, 10

198 KOH, 4 NaCl, 10 HEPES, 28.5 Sucrose, 4 Na_2ATP, 0.4 Na_3GTP, plus 0.15 % biocytin; pH ~7.3, 280-
199 290 mOsm. To study multiple action potential firing, 500 ms somatic current injections of Δ+5 pA
200 were applied from a holding potential of -60 mV in current-clamp mode with 100 % bridge balance,
201 until the point where the neuron entered depolarisation block.

202 After completion of electrophysiology experiments, the pipette was gradually removed with a small
203 amount of positive pressure applied to try and dislodge the patched neuron from the pipette. Once
204 the pipette was separated from the cell, the acute slice was transferred to 4% PFA. The slice was
205 fixed overnight at 4° C, washed with PBS (3x5 minutes) and stored in PBS and 0.05 % sodium azide at
206 4° C, for up to 3 months. Standard immunohistochemistry protocols were used (see above).
207 Streptavidin 488 (Alexa Fluor® Life Technologies) diluted 1: 1,000 was included with the secondary
208 antibodies to label biocytin in the patched neuron.

209

210 *Quantitative PCR*

211 All experimental steps for qPCR were performed in compliance with the MIQE guidelines (Bustin *et*
212 *al.*, 2009). One or 3 days after naris occlusion or control sham surgery, wild-type mice were
213 sacrificed by cervical dislocation followed by decapitation. The brain was quickly removed and
214 placed in cold PBS. The right olfactory bulb was dissected and placed in RNAlater (Ambion) overnight
215 at 4° C and stored at -20° C until further processing. Total RNA extraction was performed using the
216 RNAqueous® Micro Kit (Life Technologies). RNA was eluted in 20 µl of elusion buffer and quantified
217 using Nanodrop (Thermo Fisher Scientific) and Qubit (RNA HS Assay Kit, Life Technologies). 300-
218 500 ng of total RNA were used for cDNA synthesis with SuperScript™ II Reverse Transcriptase (Life
219 Technologies), 0.5 mM dNTPs (Life Technologies), 5 µM OligodT23VN (IDT), 10 µM DTT (Life
220 Technologies) and 0.2 Units RNase inhibitor (SUPERase•In™, Invitrogen). RNA was denatured for
221 5 min at 65° C, before adding the reaction mix. Retrotranscription was performed at 42° C for
222 90 min, followed by 20 min at 70° C for enzyme inactivation. Standard RT-PCRs were run for all
223 samples, including non-template controls, to corroborate amplification of single bands of the
224 appropriate size. Cycling conditions were: 95° C for 3 min, (95 C, 15 s; 65-55° C (-0.5° C per cycle),
225 20 s; 68° C, 25 s), 20 cycles, (95° C, 15 s; 55° C, 20 s; 68° C, 25 s), 20 cycles, 68° C, 5 min, 4° C, hold.
226 Reactions were run on a SimpliAmp™ Thermal Cycler (Applied Biosystems). Primers used were:
227 ActB_For, cctctatgccaacacagtgc; ActB_Rev, cttctgcatcctgtcagcaa; Th_For, tgcctcctcacctatgcact;
228 Th_Rev, gtcagccaacatgggtacg. Primers were designed using the Universal Probe Library Assay Design
229 Centre (Roche), compatible with UPLs 157 and 3 for ActB and Th primer pairs, respectively.

230 qPCR reactions were run using the FastStart Essential DNA Probes Master mix (Roche) on the
231 LightCycler ® 96 Real-Time PCR System (Roche). Final primer concentration was 0.5 µM and probe
232 concentration was 0.1 µM. Cycling conditions were: 95° C for 10 min, (95° C, 10 s; 60° C, 30 s),
233 55 cycles, 4° C, hold. Technical duplicates were performed for all samples and reactions.
234 Amplification efficiency for all primer pairs was determined by obtaining a standard curve. Briefly,
235 the cDNAs from each cDNA synthesis reaction were pooled and serially diluted. qPCR reactions were
236 performed as above. Ct amplification curve values were plotted as a function of dilution factor and
237 the amplification efficiency determined from the slope of the linear regression as in E = 10(-1/slope)-
238 1. Amplification efficiency for ActB primers was 1.07 ± 0.02 and for Th primers, 1.01 ± 0.03. Fold
239 changes in Th expression levels were obtained using the $2^{(-ddCt)}$ method (Livak & Schmittgen, 2001;
240 Taylor *et al.*, 2019), first normalising Th Ct levels for each sample to ActB Ct levels and subsequently
241 normalising to the average of the control (sham) conditions.

242

243 *Statistical analysis*

244 Statistical analysis was carried out using Prism (GraphPad), Matlab (Mathworks) or SPSS (IBM). All
245 datasets were described as mean ± SEM, unless otherwise stated, n values reported in the text refer
246 to number of cells, and N values refer to number of mice. Details of all individual statistical tests are
247 reported alongside the appropriate results. α values were set to 0.05 (except where a Bonferroni
248 correction was carried out for multiple comparisons) and all comparisons were two tailed. For
249 multiple group comparisons with ANOVA followed by Bonferroni post-tests, all groups either passed
250 the D'Agostino and Pearson omnibus test for normality (GraphPad Prism), and/or could be fitted by
251 a Gaussian distribution that explained ≥ 90 % of their variance (custom Matlab script written by
252 MSG). Fisher's exact test was performed when analysing proportions. Due to the design of this test,
253 data had to be analysed twice, by combining groups based on manipulation and then duration of
254 manipulation. A Bonferroni correction was therefore carried out for multiple comparisons in this
255 instance (α = 0.05/2 = 0.025). qPCR normalised TH expression data were compared with separate
256 unpaired t-tests for 1 day and 3 day samples, which also required Bonferroni correction for multiple
257 comparisons (again, α = 0.05/2 = 0.025).

258 **Results**

259

260 *Using DAT-tdTomato mice to label olfactory bulb dopaminergic neurons*

261 We used a conditional genetic strategy to label dopaminergic neurons in the olfactory bulb by
262 crossing DAT$^{IRES\,cre}$ mice (Bäckman *et al.*, 2006) with a floxed tdTomato reporter line. This resulted in
263 strong tdTomato fluorescence in small cells surrounding glomerular neuropil in the glomerular layer,
264 along with the odd scattered tdTomato-positive cell in the superficial external plexiform layer (EPL),
265 in keeping with previous reports of dopaminergic cell localisation within the olfactory bulb (Fig. 1A;
266 (e.g. Hökfelt *et al.*, 1975; Banerjee *et al.*, 2013; Kosaka *et al.*, 2019). To confirm the identity of these
267 DAT-tdTomato neurons, we co-stained fixed olfactory bulb slices from juvenile postnatal day (P)28
268 mice for the rate-limiting enzyme in the synthesis of dopamine, tyrosine hydroxylase (TH). Although
269 necessary for both dopamine and noradrenaline production, the absence of local noradrenergic cells
270 in the olfactory bulb (Hökfelt *et al.*, 1975; Rosser *et al.*, 1986) makes TH a selective marker for
271 dopaminergic neurons in this region. In control animals we found a high incidence of co-labelled
272 neurons, with ~75% of DAT-tdTomato cells staining positively for TH (Fig. 1B,C; % of tdTomato-
273 positive neurons ± SEM: TH-positive, 74 ± 4 %; TH-negative, 26 ± 4 %; n = 598 cells, N = 3; Vaaga *et*
274 *al.*, 2017). However, by no means all genetically labelled cells in the DAT-tdTomato mouse were TH-
275 positive. We reasoned that the ~25 % of non-TH-expressing DAT-tdTomato cells might be 'true'
276 dopaminergic neurons that have low, undetectable levels of TH expression due to long-term activity-
277 dependent down-regulation (e.g. Baker *et al.*, 1983). However, co-staining for another dopamine-
278 synthesising enzyme dopa decarboxylase (DDC), the expression of which is known to be resistant to
279 long-term changes in ongoing activity (Stone *et al.*, 1990; Baker *et al.*, 1993; Cave *et al.*, 2010),
280 showed that this is not the case. We found very good agreement between TH- and DDC-positive
281 cells in the olfactory bulb glomerular layer (Fig. 1B; 99 ± 0.5 % of TH-positive neurons were also DDC-
282 positive; 89 ± 2 % of DDC-positive neurons were also TH-positive; n = 598; N = 3), but we found only
283 3 % of DAT-tdTomato cells were positive for DDC without expressing TH (Fig. 1B,C; % of tdTomato-
284 positive neurons ± SEM: TH- and DDC-positive, 74 ± 4 %; DDC-positive but TH-negative, 3 ± 7 %; TH-
285 positive but DDC-negative, 0.5 ± 0.3 %; TH- and DDC-negative, 23 ± 2 %; n = 598; N = 3).

286 If ~20-25 % of DAT-tdTomato cells in the olfactory bulb are therefore non-dopaminergic, what type
287 of cell are they? Red fluorescent neurons never had the large, pear-shaped soma characteristic of
288 local excitatory neurons, the external tufted cells, in the glomerular layer (Hayar *et al.*, 2004). This
289 made them most likely to be GABAergic juxtaglomerular interneurons, which in mouse are divided
290 into three mutually exclusive subgroups expressing either TH or the calcium-binding proteins

291 calbindin and calretinin (Kohwi *et al.*, 2007; Kosaka & Kosaka, 2007; Panzanelli *et al.*, 2007; Parrish-
292 Aungst *et al.*, 2007). We never observed any DAT-tdTomato neurons that co-labelled for calbindin
293 (Fig. 1D), but we did find DAT-tdTomato cells that were positive for calretinin (Fig. 1E; Ninkovic *et al.*,
294 2010). Indeed, the tdT-positive/TH-negative subgroup was almost entirely accounted for by cells
295 expressing calretinin (Fig. 1E, F; % of tdTomato-positive neurons ± SEM: TH-positive only,
296 74.1 ± 2.24 %; calretinin-positive only, 21.71 ± 0.9 %; n = 1404; N = 3). Importantly, although we
297 observed some rare tdTomato-positive cells that were neither TH- nor calretinin-positive (Fig. 1F;
298 tdTomato-positive only, 4.2 ± 1.4%, consistent with the 3 % of tdTomato cells found above to be
299 DDC-positive but TH-negative), we never saw any tdTomato-positive cells co-labelled for both TH
300 and calretinin (n = 0 / 1404 cells from N = 3 mice). This suggests that the calretinin-positive DAT-
301 tdTomato cells are non-dopaminergic calretinin neurons that have at least transiently activated DAT
302 expression at some point in their history, rather than being dopaminergic neurons that also co-
303 express calretinin.

304 To check these cells' distinct properties, we obtained whole-cell patch-clamp recordings of DAT-
305 tdTomato neurons in acute olfactory bulb slices. Although these cells are structurally fragile and
306 extremely difficult to recover for post-recording histology (Galliano *et al.*, 2018), we were able to
307 find very rare example neurons that had been successfully filled with biocytin during our recordings
308 and then co-labelled for glomerular layer markers. While a confirmed TH-positive DAT-tdTomato
309 neuron had characteristic multiple spike production in response to a prolonged 500 ms current
310 injection in current-clamp, the one calretinin-positive tdTomato cell we managed to recover
311 displayed only a single, small spike followed by a sustained depolarised plateau potential, as
312 previously described to be typical of this bulbar cell type (Fig. 1G; Fogli Iseppe *et al.*, 2016; Benito *et*
313 *al.*, 2018). The calretinin-positive cells labelled in DAT-tdTomato mice are therefore likely to share
314 their major features with the general population of calretinin-expressing juxtaglomerular neurons.

Figure 1

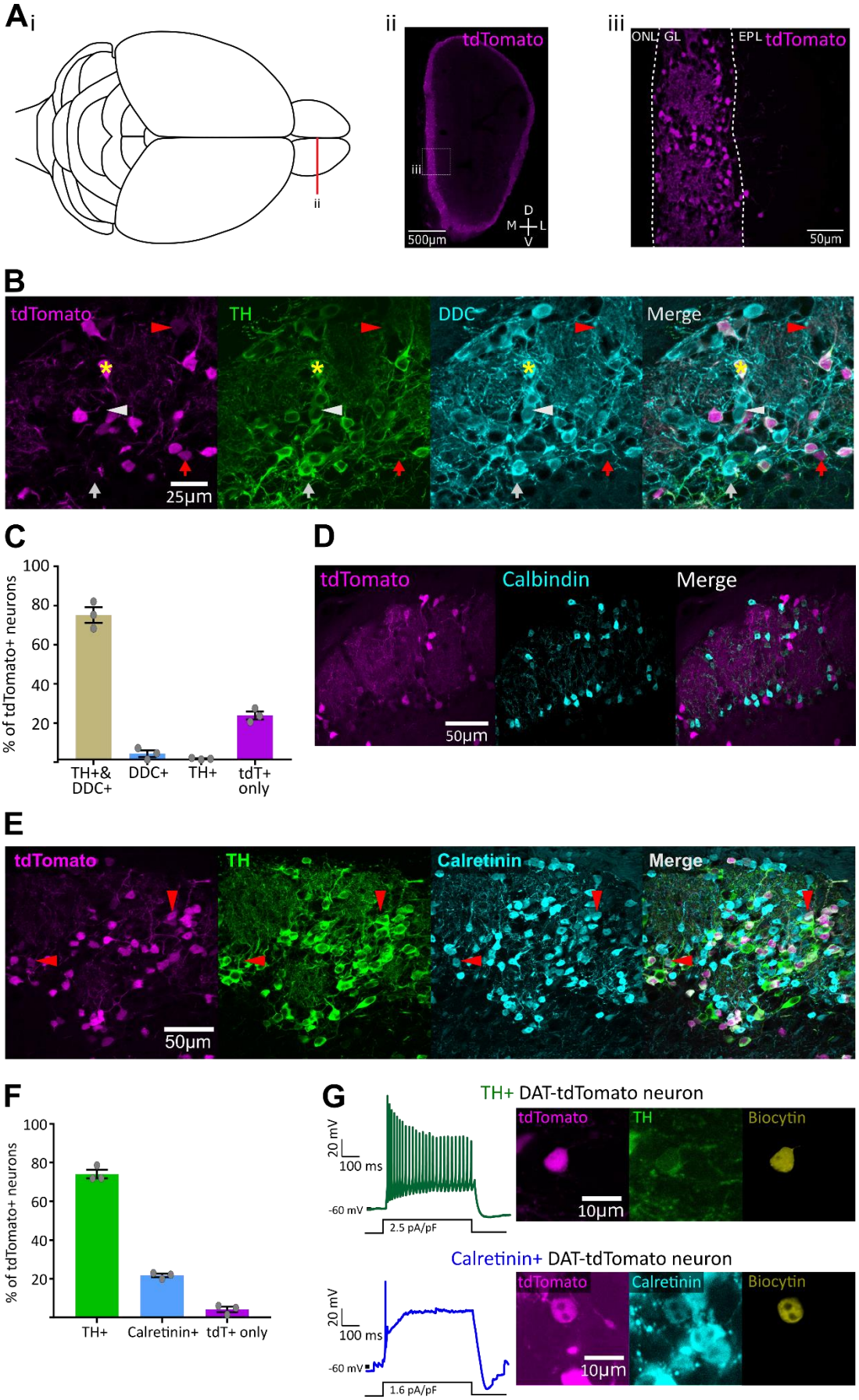
A
i
ii
iii
tdTomato
iii
500µm
D
M
L
V
ONL
GL
EPL
tdTomato
50µm
B
tdTomato
TH
DDC
Merge
25µm
C
% of tdTomato+ neurons
100
80
60
40
20
TH+& DDC+
DDC+
TH+
tdT+ only
D
tdTomato
Calbindin
Merge
50µm
E
tdTomato
TH
Calretinin
Merge
50µm
F
% of tdTomato+ neurons
100
80
60
40
20
TH+
Calretinin+
tdT+ only
G
TH+ DAT-tdTomato neuron
20 mV
100 ms
-60 mV
2.5 pA/pF
tdTomato
TH
Biocytin
10µm
Calretinin+ DAT-tdTomato neuron
20 mV
100 ms
-60 mV
1.6 pA/pF
tdTomato
Calretinin
Biocytin
10µm

317 **Figure 1**. Cell-type identity of olfactory bulb DAT-tdTomato neurons. **A)** tdTomato label in DAT-
318 tdTomato olfactory bulb; **i)** aerial view diagram of mouse brain, showing location of olfactory bulb
319 coronal section in **ii**; **ii)** coronal section of olfactory bulb from a DAT-tdTomato mouse; box shows
320 location of detail in **iii**; **iii)** tdTomato-positive neurons are located predominantly in the olfactory
321 bulb's glomerular layer (GL); ONL, olfactory nerve layer; EPL, external plexiform layer. **B)** Example
322 maximum intensity projection images from the glomerular layer in the olfactory bulb of a control
323 DAT-tdTomato mouse, showing co-label for TH and DDC. Yellow star indicates location of a neuron
324 showing expression of all three markers. Arrowheads indicate location of neurons expressing two
325 markers: red = DAT-tdTomato and DDC; white = TH and DDC. Arrows indicate location of neurons
326 expressing a single marker: red = DAT-tdTomato; white = DDC. **C)** Mean ± SEM percentage of
327 tdTomato+ neurons positive for TH and/or DDC. Grey circles indicate percentages from individual
328 mice. **D)** Example maximum intensity projection images showing immunofluorescence for calbindin
329 in the olfactory bulb glomerular layer of a control DAT-tdTomato mouse. **E)** Example maximum
330 intensity projection images showing immunofluorescence for TH and calretinin in the glomerular
331 layer of the olfactory bulb in a control DAT-tdTomato mouse. Red arrowheads indicate example
332 neurons expressing DAT-tdTomato and calretinin, but not TH. **F)** Mean ± SEM percentage of
333 tdTomato+ neurons expressing TH and calretinin. Grey circles indicate percentages from individual
334 mice. **G)** Action potential firing patterns in response to 500 ms somatic current injection (left) and
335 immunohistochemical characterisation (right) in example biocytin-filled DAT-tdTomato neurons that
336 were co-labelled for either TH (top) or calretinin (bottom).

337 *Sensory deprivation via brief unilateral naris occlusion reduces cFos expression in olfactory bulb DAT-*
338 *tdTomato neurons*

339 Having shown that the DAT-tdTomato mouse line labels olfactory bulb neurons that are
340 predominantly dopaminergic but include a distinct subset of calretinin-positive cells, we went on to
341 use this line for naturally-relevant manipulations of sensory experience (Fokkens *et al.*, 2012;
342 Galliano *et al.*, 2020). In juvenile mice from postnatal day (P)27, we induced brief 1- or 3-day periods
343 of sensory deprivation without damaging the olfactory epithelium, via unilateral naris occlusion with
344 a plastic plug (Fig.2A; Cummings *et al.*, 1997; Kikuta *et al.*, 2015; Cheetham *et al.*, 2016; Galliano *et*
345 *al.*, 2020). Because of interpretational issues caused by abnormal airflow through the contralateral
346 naris in such manipulations (Coppola, 2012; Kass *et al.*, 2013), we did not compare deprived versus
347 spared olfactory bulbs in the same animals, and instead made all comparisons between the right
348 bulbs of individual occluded or control mice (see Methods).

349 To validate the effectiveness of our sensory deprivation approach for reducing activity in olfactory
350 bulb DAT-tdTomato neurons *in vivo*, we examined immunofluorescence for the activity-dependent
351 immediate early gene cFos (Liu *et al.*, 1999). Co-embedding olfactory bulbs from all four treatment
352 groups (Fig. 2A; 1 day control, 1 day occluded; 3 day control; 3 day occluded) prior to sectioning
353 allowed the best possible consistency in immunostaining protocols (see Methods; Vlug *et al.*, 2005;
354 Galliano *et al.*, 2020). It also enabled us to normalise labelling intensity within co-embedded sets in
355 order to combine analyses across multiple individuals. With this approach we found that DAT-
356 tdTomato cells from occluded mice had significantly lower cFos immunofluorescence after both 1
357 and 3 days of occlusion (Fig. 2B-D; normalised intensity (%) mean ± SEM: 1 day control,
358 102.5 ± 3.83%, n = 316 cells, N = 2 mice; 1 day occluded, 56.85 ± 2.1%, n = 358, N = 2; 3 day control,
359 97.53 ± 3.3%, n = 317, N = 2; 3 day occluded, 62.87 ± 2.63%, n = 309, N = 2. Multi-level ANOVA
360 controlling for set variance, effect of manipulation, $F_{1,1298} = 60.73$, $p < 0.0001$; effect of time, $F_{1,1298} =$
361 1.4, $p = 0.24$; effect of manipulation x time interaction, $F_{1,1299} = 3.4$, $p = 0.07$. Bonferroni post- test
362 comparing control versus occluded ($\alpha = 0.025$): 1 day, $F_{1,673} = 115.76$, $p < 0.00005$; 3 day, $F_{1,626} =$
363 68.56, $p < 0.00005$). Brief sensory deprivation therefore reliably lowers activity levels in olfactory
364 bulb DAT-tdTomato neurons, and does so in a sustained manner over 1 to 3 days.

365 **Figure 2**

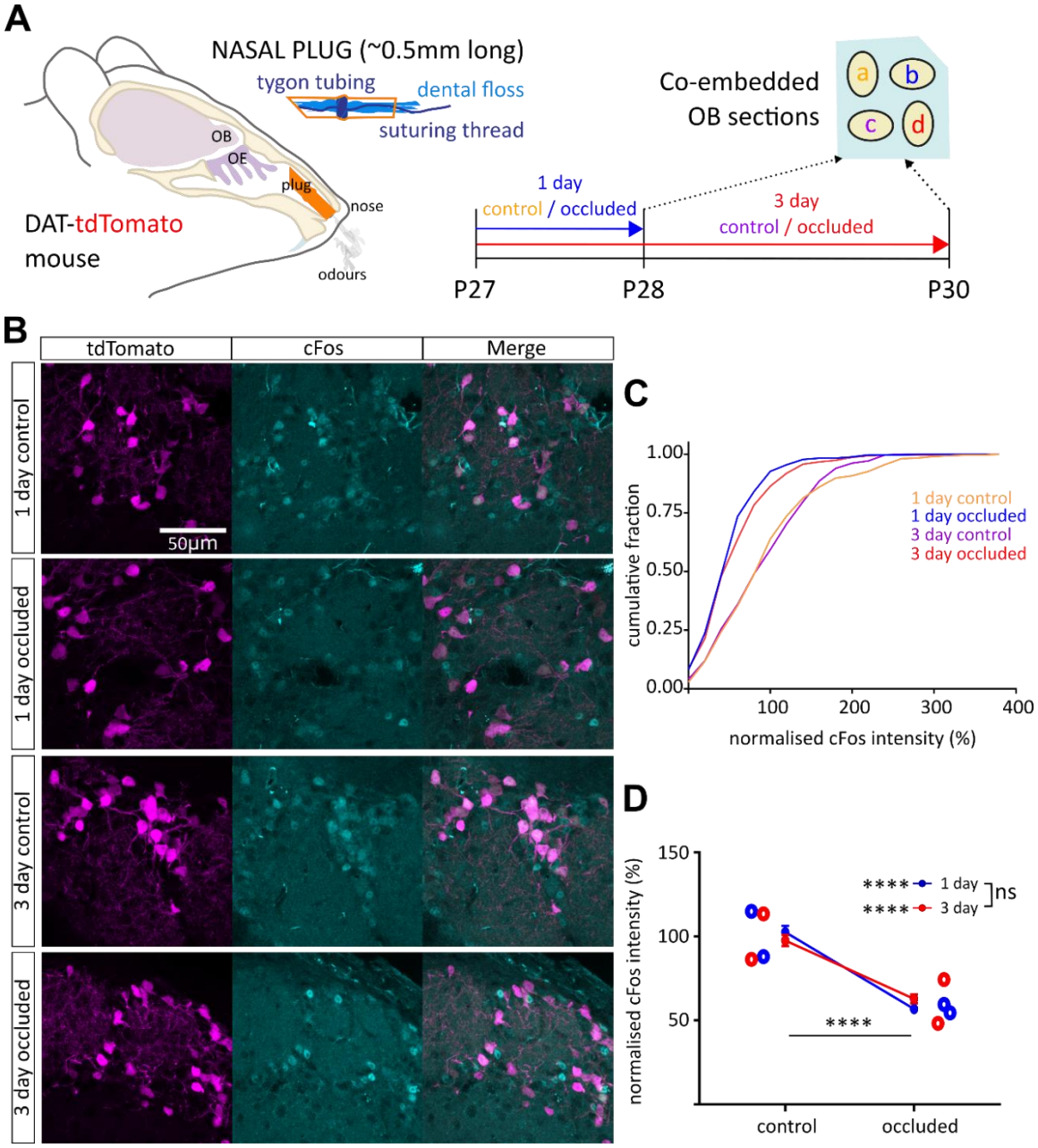

366

367 **Figure 2**. Sensory deprivation via brief unilateral naris occlusion reduces cFos expression in olfactory
368 bulb DAT-tdTomato neurons. **A)** Schematic of naris occlusion protocol and tissue co-embedding for
369 comparison of relative immunofluorescence. OE, Olfactory epithelium; OB, Olfactory bulb; P,
370 Postnatal day; a, 1 day control; b, 1 day occluded; c, 3 day control; d, 3 day occluded. **B)** Example
371 maximum intensity projection images showing immunofluorescent label for cFos in the glomerular
372 layer of the olfactory bulb in 1 and 3 day control and occluded DAT-tdTomato mice. All images are
373 from the same co-embedded preparation, acquired and presented with identical settings. **C)**
374 Cumulative distribution of normalised cFos intensity (%) in DAT-tdTomato neurons in each treatment
375 group. **D)** Line plots showing overall mean ± SEM normalised cFos intensity (%) in each treatment
376 group; unfilled circles show mean normalised cFos intensity (%) for individual mice. Multi-level
377 ANOVA controlling for set variance; effect of manipulation, **** $p < 0.0001$; effect of time, ns: non-
378 significant. Bonferroni post-test ($\alpha = 0.025$); 1 day, effect of manipulation, **** $p < 0.00005$; 3 day,
379 effect of manipulation, **** $p < 0.00005$.

380 *Brief naris occlusion does not alter the sub-type composition of olfactory bulb DAT-tdTomato neurons*

381 Given the mixed dopaminergic and calretinin-expressing nature of the population labelled in the
382 DAT-tdTomato mouse olfactory bulb (Fig. 1), it was important to check whether our effective short-
383 term sensory manipulations (Fig. 2) altered this sub-type composition in any way. Crucially, we
384 found no change in the proportion of DAT-tdTomato cells that were calretinin-positive after 1 or 3
385 days of sensory deprivation (Fig. 3A,B; % of calretinin-positive DAT-tdTomato neurons; 1 day control,
386 20.95 %, n = 506, N = 3; 1 day occluded, 24.5 %, n = 502, N = 3; 3 day control, 23.91 %, n = 343, N = 2;
387 3 day occluded, 25 %, n = 424, N = 3. Fisher's exact test with $\alpha = 0.025$, effect of manipulation, $p =$
388 0.22; effect of time, $p = 0.40$).

389 Olfactory bulb dopaminergic neurons are not a unitary, homogeneous cell type (Galliano *et al.*, 2018;
390 Kosaka *et al.*, 2019), so it was also important to assess the representation of dopaminergic subtypes
391 amongst DAT-tdTomato neurons following sensory deprivation. Work from our laboratory and
392 others has identified a key distinction between, on the one hand, small-soma olfactory bulb
393 dopaminergic cells that lack an axon and can be generated throughout life and, on the other, large-
394 soma olfactory bulb dopaminergic cells that possess an axon and are exclusively generated in early
395 embryonic development (Galliano *et al.*, 2018; Kosaka *et al.*, 2019). The latter large-soma sub-
396 population, although present, is significantly under-represented by DAT-tdTomato label, which is
397 dominated by small-soma anaxonic cells (Galliano *et al.*, 2018). Using a previously established soma
398 area cut-off value of 70 μm^2 to define olfactory bulb dopaminergic cells as 'small' (Galliano *et al.*,
399 2018), we confirmed here that this subtype accounts for > 90 % of DAT-tdTomato neurons
400 (Fig.3C,D). Crucially, the high proportion of such small cells represented in the DAT-tdTomato line –
401 which will also include the small-soma calretinin-positive subgroup (Parrish-Aungst *et al.*, 2007) –
402 was not significantly affected by 1 or 3 day naris occlusion (Fig.3C,D; % of 'small' cells; 1 day control,
403 95.22 %, n = 460, N = 3; 1 day occluded, 91.18 %, n = 408, N = 3; 3 day control, 93.62 %, n = 298, N =
404 2; 3 day occluded, 96.75 %, n = 461, N = 3. Fisher's exact test with $\alpha = 0.025$, effect of manipulation,
405 $p = 0.75$; effect of time, $p = 0.067$). Brief periods of sensory deprivation therefore do not
406 significantly alter the cellular sub-composition of olfactory bulb glomerular layer neurons labelled in
407 DAT-tdTomato mice.

408 **Figure 3**

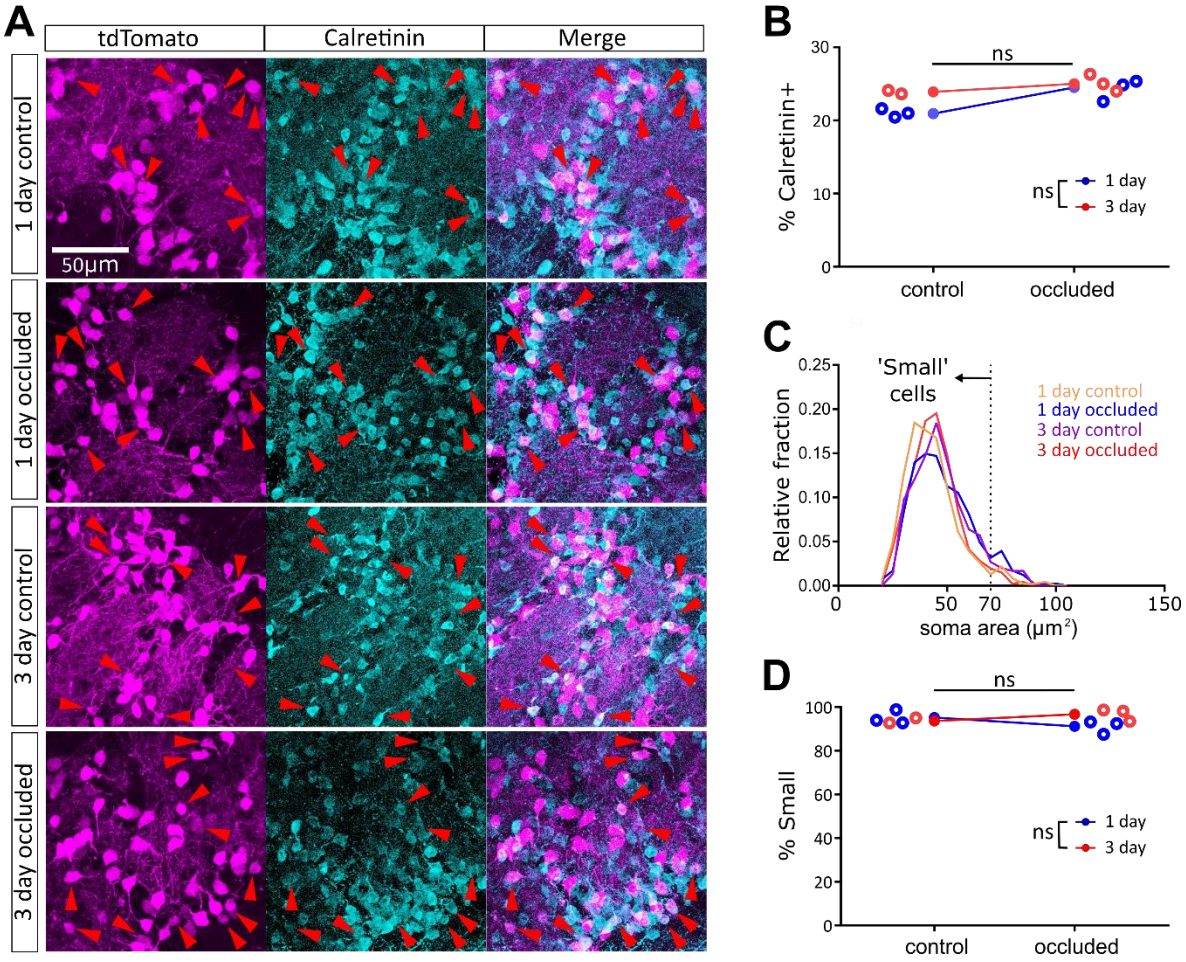

409

410 **Figure 3**. Brief naris occlusion does not alter the sub-type composition of olfactory bulb DAT-
411 tdTomato neurons. **A)** Example maximum intensity projection images showing immunofluorescence
412 for tdTomato and calretinin in the glomerular layer of the olfactory bulb in 1 and 3 day control and
413 occluded DAT-tdTomato mice. Red arrowheads indicate example neurons co-expressing
414 DAT-tdTomato and calretinin. **B)** Line plots showing, for each treatment group, overall % of
415 tdTomato+ neurons that also express calretinin. Open circles show % values for individual mice.
416 Fisher's exact test with Bonferroni correction for multiple comparisons ($\alpha = 0.025$); ns, non-
417 significant. **C)** Histogram of soma sizes for all tdTomato+ neurons in each treatment condition.
418 Dotted line shows 70 μm^2 threshold for cells classed as 'small'. **D)** Small cell % data; all conventions
419 as in **B**.

420 *Brief sensory deprivation does not affect GAD67 expression in olfactory bulb DAT-tdTomato neurons*

421 Having confirmed that brief unilateral naris occlusion effectively lowers activity levels in the
422 olfactory bulb DAT-tdTomato population without affecting its subtype composition, we used this
423 mouse line to investigate potential experience-dependent plasticity in the expression of
424 neurotransmitter-synthesising enzymes. We focused first on the GABA-synthesising enzyme isoform
425 GAD67, which is ubiquitously expressed in dual GABA- and dopamine-releasing olfactory bulb
426 neurons (Kosaka & Kosaka, 2007; Kiyokage *et al.*, 2010; Kosaka *et al.*, 2019), and has been previously
427 reported to undergo experience-dependent changes in both mRNA expression and protein levels
428 after prolonged manipulations (Parrish-Aungst *et al.*, 2011; Lau & Murthy, 2012; Banerjee *et al.*,
429 2013; Wang *et al.*, 2017). However, here we found no changes in relative GAD67
430 immunofluorescence intensity in olfactory bulb DAT-tdTomato neurons after 1 or 3 days of unilateral
431 naris occlusion (Fig.4; normalised immunofluorescence intensity (%) mean ± SEM: 1 day control,
432 97.43 ± 3.1 %, n = 261, N = 3; 1 day occluded, 92.93 ± 2.9 %, n = 314, N = 3; 3 day control, 103.5 ±
433 3.7 %, n = 192, N = 2; 3 day occluded, 94.03 ± 2.88 %, n = 304, N = 3. Multi-level ANOVA controlling
434 for set variance, effect of manipulation, $F_{1,1071} = 0.09$, $p = 0.77$; effect of time, $F_{1,1071} = 1.6$, $p = 0.21$;
435 effect of manipulation x time interaction, $F_{1,1071} = 0.62$, $p = 0.43$).

436 **Figure 4**

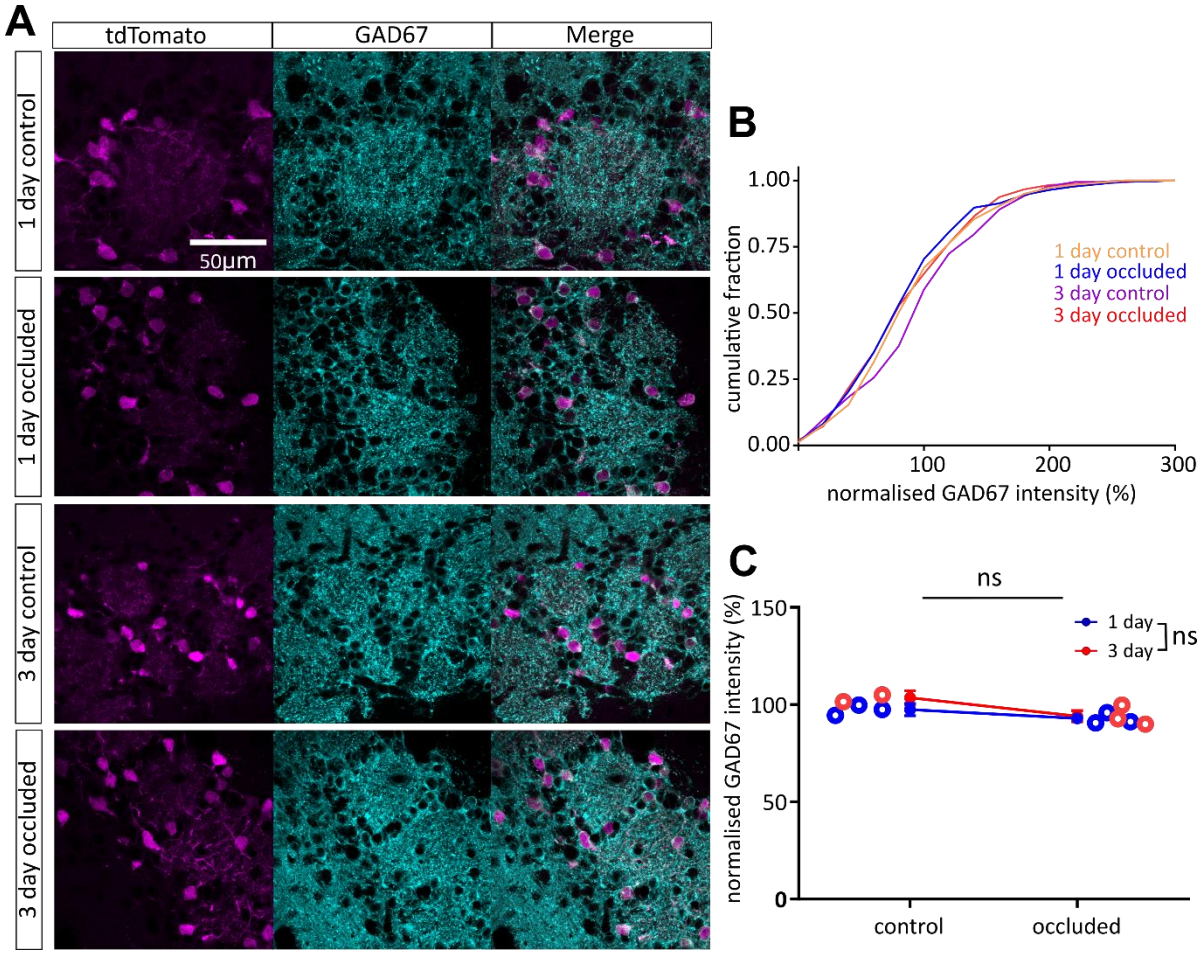

437

438 **Figure 4**. Brief sensory deprivation does not affect GAD67 expression in olfactory bulb DAT-
439 tdTomato neurons. **A)** Example maximum intensity projection images showing immunofluorescence
440 for GAD67 in the glomerular layer of the olfactory bulb in 1 and 3 day control and occluded DAT-
441 tdTomato mice. All images are from the same co-embedded preparation, acquired and presented
442 with identical settings. **B)** Cumulative distribution of normalised GAD67 intensity (%) in DAT-
443 tdTomato neurons in each treatment group. **C)** Line plots showing overall mean ± SEM of
444 normalised GAD67 intensity (%) in each treatment group; unfilled circles show mean normalised
445 GAD67 intensity (%) for individual mice. Multi-level ANOVA controlling for set variance; effect of
446 manipulation and effect of time, ns: non-significant.

447 *DDC expression in olfactory bulb DAT-tdTomato neurons is only slightly and transiently reduced by*
448 *unilateral naris occlusion*

449 The enzyme DDC catalyses the direct synthesis of dopamine from L-DOPA, but unlike TH has
450 received relatively little attention regarding its potential for activity-dependent expression. Indeed,
451 two previous studies found no effect of odour deprivation on *Ddc* mRNA levels in the olfactory bulb
452 following prolonged, >1 month-long naris closure (Stone *et al.*, 1990; Cave *et al.*, 2010). Here, we
453 found that brief sensory deprivation produced a small but significant decrease in the relative
454 immunofluorescence intensity of DDC in olfactory bulb DAT-tdTomato neurons (Fig. 5; normalised
455 immunofluorescence intensity (%) mean ± SEM: 1 day control, 97.99 ± 2.61%, n = 417, N = 2; 1 day
456 occluded, 82.88 ± 2.47%, n = 425, N = 2; 3 day control, 104.2 ± 3.45%, n = 198, N = 1; 3 day occluded,
457 96.03 ± 2.61%, n = 412, N = 2. Multi-level ANOVA controlling for set variance, effect of manipulation,
458 $F_{1,1452} = 10.19$, $p = 0.001$; effect of time, $F_{1,1452} = 1.95$, $p = 0.16$; effect of manipulation x time
459 interaction, $F_{1,1452} = 1.44$, $p = 0.22$). Post-hoc tests demonstrated that this effect was driven largely
460 by a reduction in DDC immunofluorescence only after 1 day of occlusion, with expression of DDC in 3
461 day occluded DAT-tdTomato neurons returning back close to control levels (Fig. 5C; Bonferroni post-
462 test comparing control versus occluded with $\alpha = 0.025$: 1 day, $F_{1,842} = 17.70$, $p < 0.0001$; 3 day, $F_{1,610} =$
463 3.39, $p = 0.066$). Small and transient changes in relative DDC levels are therefore possible in
464 olfactory bulb dopaminergic cells experiencing sustained decreases in activity.

465 **Figure 5**

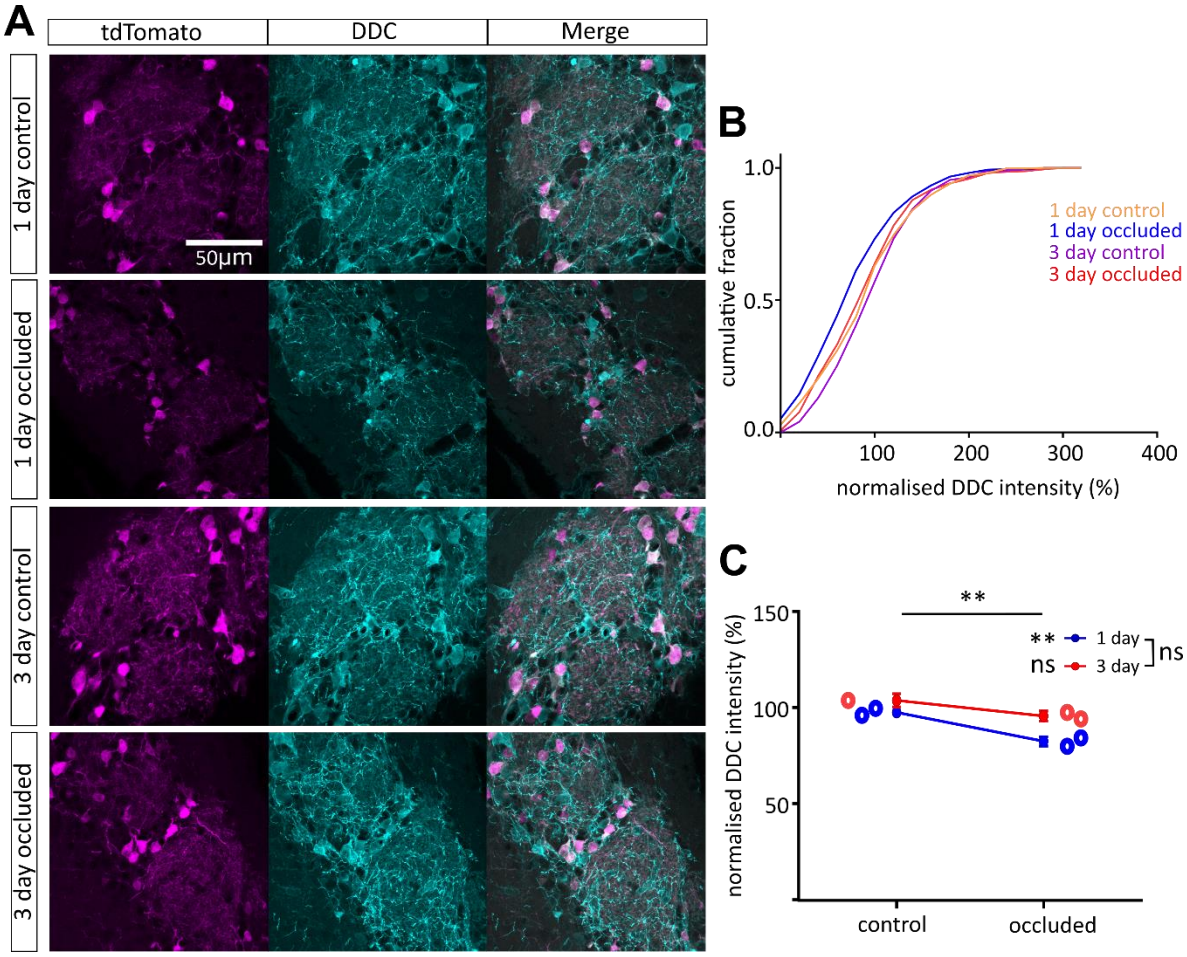

466

467 **Figure 5**. DDC expression in olfactory bulb DAT-tdTomato neurons is slightly reduced only after
468 1 day of unilateral naris occlusion. **A)** Example maximum intensity projection images showing
469 immunofluorescence for DDC in the glomerular layer of the olfactory bulb in 1 and 3 day control and
470 occluded DAT-tdTomato mice. All images are from the same co-embedded preparation, acquired
471 and presented with identical settings. **B)** Cumulative distribution of normalised DDC intensity (%) in
472 DAT-tdTomato neurons in each treatment group. **C)** Line plots showing overall mean ± SEM of
473 normalised DDC intensity (%) in each treatment group; unfilled circles show mean normalised DDC
474 intensity (%) for individual mice. Multi-level ANOVA controlling for set variance; effect of
475 manipulation, ** $p < 0.01$; effect of time, ns: non-significant. Bonferroni post-test ($\alpha = 0.025$); 1 day,
476 effect of manipulation, ** $p < 0.005$; 3 day, effect of manipulation, ns: non-significant.

477 *Brief sensory deprivation reduces TH expression in olfactory bulb DAT-tdTomato neurons*

478 Olfactory bulb dopaminergic neurons have a well-described ability to regulate TH expression in an
479 activity-dependent manner, including after unilateral naris occlusion by plug insertion (Nadi *et al.*,
480 1981; Baker *et al.*, 1983; Kosaka *et al.*, 1987; Cummings *et al.*, 1997). The most rapid previously-
481 published example of this found that 2 days of odour deprivation induced a small, but significant,
482 decrease in *Th* mRNA in the occluded olfactory bulb compared to open-side control (Cho *et al.*,
483 1996). In cultured bulbar neurons or slices, however, just one day of elevated activity was sufficient
484 to increase TH immunofluorescence intensity or TH-GFP transgene expression (Akiba *et al.*, 2007;
485 Chand *et al.*, 2015). We also recently found that 24 h naris occlusion was accompanied by a
486 significant drop in immunofluorescence for TH in the ipsilateral olfactory bulb, without producing a
487 change in TH-positive cell density (Galliano *et al.*, 2020). However, the above approaches had the
488 drawback that they used TH expression itself as a means to identify samples for TH quantification.
489 We therefore used our conditional genetic labelling strategy to assess rapid deprivation-induced
490 changes in TH expression in an independently identified neuronal population.

491 Brief sensory deprivation was indeed associated with a decrease in the relative intensity of TH
492 immunofluorescence in olfactory bulb DAT tdTomato neurons (Fig.6A-C; normalised
493 immunofluorescence intensity (%) mean ± SEM: 1 day control, 95.27 ± 3.35%, n = 460, N = 3; 1 day
494 occluded, 70.96 ± 3.16%, n = 408, N = 3; 3 day control, 107.3 ± 4.64%, n = 298, N = 2; 3 day occluded,
495 57 ± 2.32%, n = 461, N = 3. Multi-level ANOVA controlling for set variance, effect of manipulation,
496 $F_{1,1546.} = 2.9$, $p = 0.09$; effect of time, $F_{1,1626} = 3.1$, $p = 0.08$). This effect was highly significant after just
497 1 day (Fig. 6C; Bonferroni post-test comparing control versus occluded with $\alpha = 0.025$: 1 day, $F_{1,867} =$
498 27.41, $p < 0.00005$), but was even stronger after 3 days (Fig. 6C; post-test: 3 day, $F_{1,639} = 76.36$, $p <$
499 0.00005; effect of manipulation x time interaction in main ANOVA, $F_{1,1613} = 11.67$, $p = 0.001$).
500 Continuous naris occlusion therefore produces a rapid downregulation in TH immunofluorescence in
501 independently identified olfactory bulb dopaminergic neurons, and this effect becomes stronger
502 over time.

503 Finally, we also observed rapid occlusion-induced downregulation of *Th* expression at the mRNA
504 level, as assessed via qPCR on whole-OB samples from wild-type mice. Compared to sham-treated
505 bulbs, OBs on the occluded side had significantly lower levels of Th expression after both 1 day and
506 3 days of sensory deprivation (Fig.6D; 1 day mean ± SEM fold change: sham, 1.02 ± 0.07; occluded,
507 0.66 ± 0.04; t-test with $\alpha = 0.025$, $t_{18} = 4.69$, $p = 0.0002$, N = 20; 3 day: sham, 1.04 ± 0.13; occluded,
508 0.53 ± 0.03; Welch's t-test with $\alpha = 0.025$, $t_{7.73} = 4.00$, $p = 0.0043$; N = 16).

509 **Figure 6**

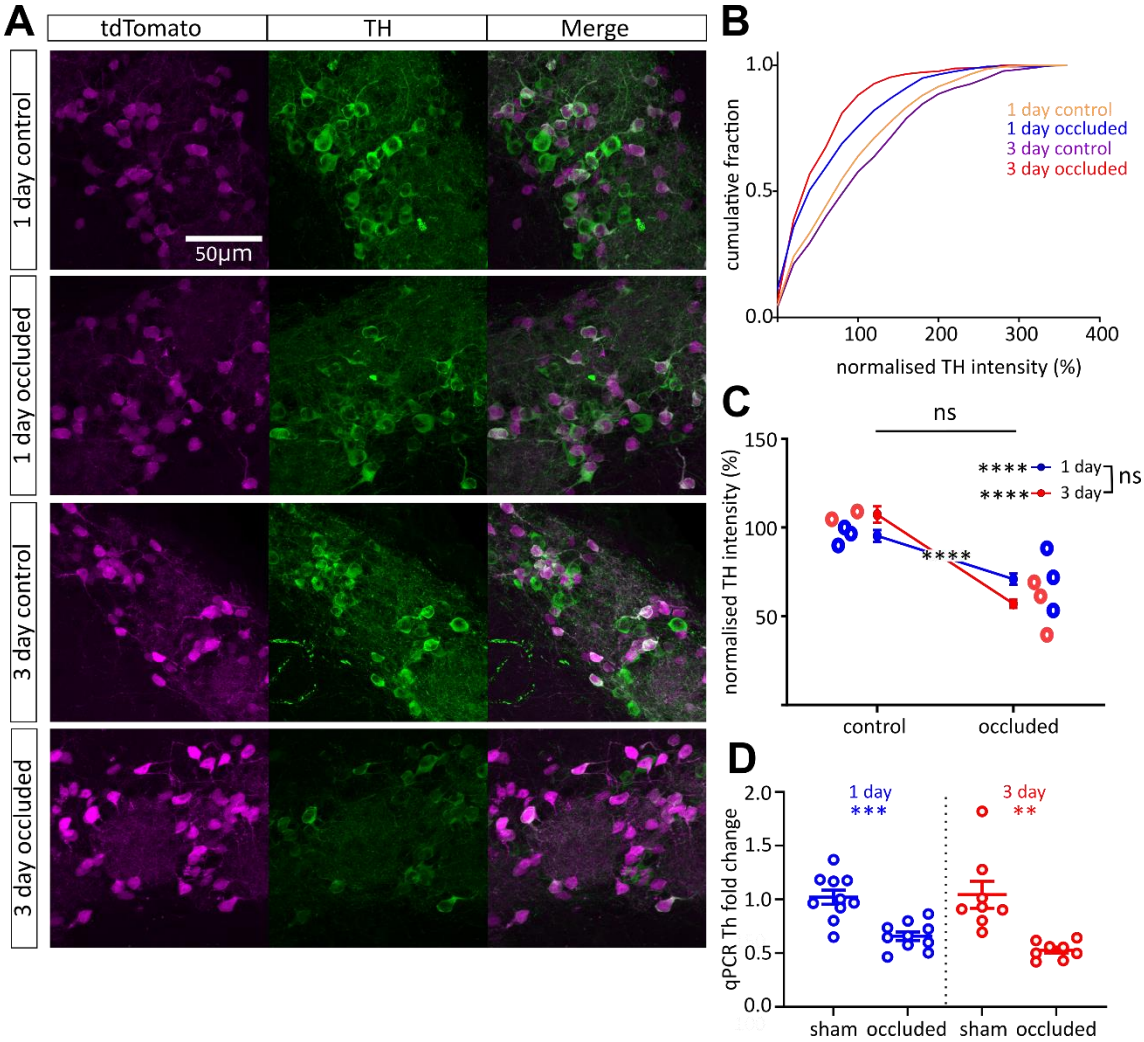

510

511 **Figure 6**. Brief sensory deprivation reduces TH expression in olfactory bulb DAT-tdTomato neurons.
512 **A)** Example maximum intensity projection images showing immunofluorescence for TH in the
513 glomerular layer of the olfactory bulb in 1 and 3 day control and occluded DAT-tdTomato mice. All
514 images are from the same co-embedded preparation, acquired and presented with identical
515 settings. **B)** Cumulative distribution of normalised TH intensity (%) in DAT-tdTomato neurons in each
516 treatment group. **C)** Line plots showing overall mean ± SEM of normalised TH intensity (%) in each
517 treatment group; unfilled circles show mean normalised TH intensity (%) for individual mice. Multi-
518 level ANOVA controlling for set variance; effect of manipulation x time interaction, **** $p < 0.0001$;
519 effect of manipulation and effect of time, ns: non-significant. Bonferroni post-test ($\alpha = 0.025$); 1 day,
520 effect of manipulation, **** $p < 0.00005$; 3 day, effect of manipulation, **** $p < 0.00005$. **D)** *Th*
521 mRNA expression by whole-bulb qPCR. Circles show fold change for individual bulbs vs relevant
522 sham control mean; lines show mean ± SEM fold change for each group. t-test ($\alpha = 0.025$); 1 day,
523 ***, $p = 0.0002$; 3 day, **, $p = 0.0043$.

524 **Discussion**

525

526 Here we used a conditional genetic strategy to identify olfactory bulb neurons expressing the
527 dopamine transporter. DAT-tdTomato neurons were predominantly dopaminergic, but also included
528 a subset of non-dopaminergic, calretinin-positive cells. Importantly, while the activity of DAT-
529 tdTomato cells could be readily manipulated with brief periods of sensory deprivation, these
530 manipulations did not alter the labelled neurons' subtype composition. We found that 1-3 days of
531 unilateral naris occlusion was insufficient to alter relative levels of immunolabel for the GABA-
532 synthesising enzyme GAD67 in these cells. In contrast, similarly brief sensory manipulations were
533 associated with significant activity-dependent changes in the levels of enzymes required for the
534 synthesis of dopamine.

535

536 *Identifying olfactory bulb dopaminergic neurons using DAT$^{IRES\mathrm{cre}}$ mice*

537 Using transgenic approaches to label specific cell types in the brain requires thorough
538 characterisation of their specificity. To study dopaminergic neurons in the olfactory bulb, several
539 previous studies have utilised conditional or knock-in strategies based on expression driven from the
540 *Th* promoter (e.g. Saino-Saito *et al.*, 2004; Pignatelli *et al.*, 2005; Kiyokage *et al.*, 2010; Adam &
541 Mizrahi, 2011; Liu *et al.*, 2013; Wachowiak *et al.*, 2013). However, *Th* mRNA expression is more
542 widespread than TH protein expression in the bulb, with the former being observed amongst
543 presumptive immature migrating neurons, as well as amongst TH-immunopositive neurons
544 concentrated in the glomerular layer (Saino-Saito *et al.*, 2004; Pignatelli *et al.*, 2009; Banerjee *et al.*,
545 2013). In other brain regions, the specificity of TH-Cre mice for labelling dopaminergic neurons also
546 appears to be rather low (Lammel *et al.*, 2015). We therefore opted for a conditional genetic
547 labelling strategy based on Cre recombinase expression under the control of the DAT promoter,
548 which has been reported to be more specific to TH-positive neurons in general (Lammel *et al.*, 2015),
549 and which has already been used successfully to target olfactory bulb dopaminergic neurons. In
550 those bulb studies, which either employed the DAT$^{\mathrm{IRES}cre}$ line used here (Vaaga *et al.*, 2017; Short &
551 Wachowiak, 2019; Sato *et al.*, 2020) a DAT-Cre knock-in model (Ninkovic *et al.*, 2010; Banerjee *et al.*,
552 2015), or a BAC transgenic DAT-CreER^{T2} inducible line (Bywalez *et al.*, 2016), approximately 85% of
553 genetically-labelled neurons were found to be TH-positive by immunohistochemistry (Banerjee *et*
554 *al.*, 2015; Vaaga *et al.*, 2017). This is broadly in line with the ~75% co-label we found here, with
555 cross-study variability possibly arising from differences in the Cre-dependent reporter lines utilised

556 and/or differences in label detection criteria. Nevertheless, the general approach of using DAT-Cre
557 mice to label dopaminergic neurons in the olfactory bulb clearly produces reasonable specificity.

558 However, we found that not all DAT-tdTomato olfactory bulb cells were TH-positive, and that the
559 large majority of non-dopaminergic genetically labelled neurons (~20 %) expressed the calcium-
560 binding protein calretinin. Calretinin expression in DAT-Cre-positive bulbar neurons has been
561 previously reported, but not quantified, in a separate knock-in line (Ninkovic *et al.*, 2010). This
562 suggests that off-target label of calretinin cells is not a peculiarity of one particular genetic
563 manipulation, but instead reflects a biological link between these neurons and their dopaminergic
564 neighbours. Indeed, fate mapping neuronal precursors that generate glomerular layer GABAergic
565 interneurons has demonstrated that the decision to differentiate into a dopaminergic neuron over a
566 calretinin neuron relies on just a few transcription factors. Loss of Pax6, Dlx2 or Meis2 reduces the
567 proportion of postnatal dopaminergic neurons that are generated, while increasing the number of
568 calretinin neurons (Brill *et al.*, 2008; Agoston *et al.*, 2014). Overexpression of Dlx2 increases the
569 proportion of dopaminergic neurons and decreases the calretinin population (Brill *et al.*, 2008). The
570 transcription factor Er81 is also expressed in both calretinin and dopaminergic neurons in the
571 glomerular layer and is important in mice for regulating the expression of *Th* (Cave *et al.*, 2010).
572 Therefore, the molecular determinants of dopaminergic versus calretinin identities appear to be
573 closely interdependent. It remains unclear whether tdTomato expression in some calretinin neurons
574 is due to transient expression of DAT during their development, or whether this subset of cells
575 continues to express DAT postnatally. In the former case, obtaining transgenic label via inducible
576 activation of DAT-Cre in mature mice (Bywalez *et al.*, 2016) might result in greater specificity for
577 bulbar dopaminergic neurons. Low levels of bulbar DAT expression (Cockerham *et al.*, 2016)
578 unfortunately precluded us from addressing this question using immunohistochemistry, but targeted
579 interrogation of single-cell sequencing datasets (e.g. Zeisel *et al.*, 2018) might provide an answer in
580 the near future. Regardless, it is clear that this minority calretinin-expressing population needs to be
581 considered when interpreting the results of experiments performed on 'dopaminergic' neurons
582 targeted via DAT-Cre mouse lines (Wachowiak *et al.*, 2013; Banerjee *et al.*, 2015; Bywalez *et al.*,
583 2016; Vaaga *et al.*, 2017; Galliano *et al.*, 2018, 2020; Sato *et al.*, 2020). Thankfully, though, the
584 distinct and unusually immature-like properties of glomerular layer calretinin-positive cells, including
585 their extremely low excitability and apparent lack of GABA release (Fogli Iseppe *et al.*, 2016; Benito
586 *et al.*, 2018; Tavakoli *et al.*, 2018), mean that their presence as a minority of DAT-Cre-targeted cells is
587 unlikely to have significantly biased the conclusions of those previous studies.

588 Our main goal was to achieve reasonable specificity in genetically labelling olfactory bulb
589 dopaminergic neurons, but we note that our approach was by no means comprehensive in labelling

590 *all* olfactory bulb dopaminergic neurons. As is the case for many Cre lines (Heffner *et al.*, 2012), we
591 saw mosaicism in the fact that many immunohistochemically-defined TH-positive neurons did not
592 express the tdTomato marker (see Fig. 1B,E; % of TH-positive neurons that were tdTomato-negative,
593 36 ± 0.2 %, n = 692 cells, N = 3 mice; Galliano *et al.*, 2018). The DAT$^{IRES\,cre}$ line is also known to
594 particularly under-represent one subtype of bulbar dopaminergic neuron – the large-soma, axon-
595 bearing, embryonically-generated subclass (Galliano *et al.*, 2018) – and we found again here that
596 small-soma, presumed anaxonic neurons dominate the tdT-labelled population. However, large-
597 soma, axon-positive cells are already rare amongst the olfactory bulb dopaminergic population, and
598 they can certainly still be labelled in DAT-tdTomato mice (Galliano *et al.*, 2018). So, although the
599 DAT$^{IRES\,cre}$ line produces genetic label which is heavily biased towards one particular dopaminergic
600 subpopulation in the olfactory bulb, it is far from being entirely subtype specific. Overall, the
601 strategy of using DAT-based transgenic lines to target dopaminergic neurons in the olfactory bulb
602 can produce good levels of specificity, but care needs to be taken to fully characterise the resulting
603 label before such experiments can be safely interpreted.

604

605 *Experience-dependent plasticity of GAD67*

606 With brief periods of sensory deprivation, we saw no evidence here for changes in relative GAD67
607 immunofluorescence amongst olfactory bulb DAT-tdTomato-expressing neurons. Given the mixed
608 calretinin- and TH-positive composition of our tdTomato-labelled population (Fig. 1), this result could
609 theoretically have been produced if changes in GAD67 levels in dopaminergic neurons were
610 perfectly offset by inverse, and stronger, changes in the smaller calretinin-positive tdTomato
611 subgroup. We did not co-label for calretinin and GAD67 in this study, while the literature contains
612 conflicting reports as to whether calretinin-positive neurons in the olfactory bulb express GAD67 at
613 all (Panzanelli *et al.*, 2007; Parrish-Aungst *et al.*, 2007; opposing results are likely due to the different
614 transgenic versus immunohistochemical labelling methods employed in these studies). Even if
615 calretinin-positive tdTomato cells do express GAD67, however, the most parsimonious
616 interpretation of our data remains that dopaminergic bulbar neurons do not rapidly alter their
617 GAD67 levels in response to sensory deprivation. This fits with previous work measuring general
618 GAD (i.e. GAD65+67) expression in the bulb, which found no significant alterations following more
619 long-term sensory deprivation (Kosaka *et al.*, 1987; Stone *et al.*, 1991; Baker *et al.*, 1993). In contrast,
620 reduced expression of GAD67, but not GAD65, has been observed after 7 days of unilateral naris
621 occlusion and deafferentation via measures of glomerular layer immunofluorescence and whole-
622 bulb protein expression (Parrish-Aungst *et al.*, 2011). Decreased expression of *Gad1* mRNA and

623 GAD67 protein have also been described following chemical ablation of olfactory sensory neurons
624 (Lau & Murthy, 2012) or unilateral naris occlusion (Banerjee *et al.*, 2013; Wang *et al.*, 2017).
625 However, these studies used longer-duration manipulations and did not distinguish between
626 different bulbar neuronal populations. Therefore, either 1-3 days of unilateral naris occlusion is
627 insufficient to induce activity dependent changes in GAD67, or measures based on
628 immunofluorescence intensity may not be sensitive enough to always detect changes in GAD67, or
629 these changes are driven in neurons not labelled in the DAT-tdTomato mouse line.

630

631 *Experience-dependent plasticity of dopamine-synthesising enzymes*

632 We report here the first description of activity-dependent changes in olfactory bulb DDC levels. This
633 effect was small and transient, with relative DDC immunofluorescence in DAT-tdTomato neurons
634 returning back to baseline after just 3 days of sensory deprivation. Such temporary downregulation
635 might explain why previous studies – which used much longer periods of sensory manipulation - did
636 not find similar effects (Stone *et al.*, 1990; Cave *et al.*, 2010), although expression of DDC in the
637 midbrain has been reported to be affected within a few hours of activation or blockade of dopamine
638 receptors (Hadjiconstantinou *et al.*, 1993; Zhu *et al.*, 1993). Further work is needed to confirm
639 whether downregulation of bulbar DDC after 1 day of occlusion is a consistent activity-dependent
640 modification. If so, it might reflect an initial strategy whereby dopaminergic neurons downregulate
641 multiple nodes in the dopamine synthesis pathway, before sufficiently decreased TH activity can
642 alone – as the rate-limiting step – control levels of transmitter production.

643 Our data showing decreased TH expression after olfactory sensory deprivation are entirely
644 consistent with a large body of prior work describing this effect (Nadi *et al.*, 1981; Baker *et al.*, 1983,
645 1984, 1993, 1999; Kosaka *et al.*, 1987; Baker, 1990; Stone *et al.*, 1990; Cho *et al.*, 1996; Philpot *et al.*,
646 1998; Saino-Saito *et al.*, 2004; Bastien-Dionne *et al.*, 2010; Cave *et al.*, 2010; Weiss *et al.*, 2011; Grier
647 *et al.*, 2016), including some indications that it can occur after relatively brief manipulations (Cho *et*
648 *al.*, 1996; Akiba *et al.*, 2007; Chand *et al.*, 2015; Galliano *et al.*, 2020). It is novel, however, that our
649 methodological approach demonstrated activity-dependent TH alterations in cells identified in an
650 entirely TH-independent manner. As discussed above, this approach was not completely selective,
651 labelling a minority of calretinin-positive neurons in addition to dopaminergic cells. However, since
652 we never observed a DAT-tdTomato neuron that was both calretinin-positive and dopaminergic, and
653 since the proportions of calretinin-positive cells did not change significantly with occlusion (Fig. 3),
654 this off-target labelled sub-population cannot account for the relative changes in TH and DDC
655 immunofluorescence we observed. Indeed, if anything, the presence of a significant proportion of

656 essentially TH- or DDC-negative cells amongst the DAT-tdTomato samples we analysed may have
657 made our ability to detect relative differences in enzyme levels less sensitive.

658 We also note the caveat that, of course, changes in immunofluorescence intensity cannot be used to
659 infer activity-dependent plasticity in *absolute* levels of protein expression. With this approach,
660 results can be easily confounded by variability in the duration of immunohistochemistry steps, the
661 composition of reagents, and/or individual image acquisition settings. We did take every possible
662 measure to mitigate against such factors, comparing tissue from mice that were fixed on the same
663 day with the same fixative solution, comparing sections that were physically co-embedded prior to
664 all stages of histological processing, and comparing images that were taken on the same day with
665 the same acquisition settings. We also ensured that we only ever made *relative* comparisons of
666 immunofluorescence. So, while we are confident that, for example, TH levels decreased in DAT-
667 tdTomato cells after 1 day of sensory deprivation, we do not claim any insight into the magnitude of
668 this decrease. We do, however, have corroborative, fully quantitative qPCR data to show that – at
669 least at the whole-bulb level – brief sensory deprivation is associated with an approximate halving of
670 TH mRNA levels.

671

672 *Mechanisms*

673 It remains unclear precisely how activity-dependent changes in TH expression occur, though the
674 immediate depolarisation-activated pathways appear to require signalling through L-type CaV1
675 Channels and cAMP (Cigola *et al.*, 1998), and *Th* gene expression is at least partly controlled by
676 changes in secondary DNA structure influencing the binding of heterogeneous nuclear
677 ribonucleoproteins (hnRNPs) to its proximal promoter (Banerjee *et al.*, 2014; Wang *et al.*, 2017). Our
678 findings suggest that these processes can work over reasonably quick timescales. However, given
679 the similarity in promoter-based changes in secondary structure and hnRNP binding between the *Th*
680 and *Gad1* genes (Wang et al., 2017), it will be interesting to consider how these processes can work
681 more rapidly, more specifically, and/or be coupled with targeted changes in mRNA and protein
682 turnover, to produce selective downregulation of TH without any changes in GAD67 after a few days
683 of naris occlusion.

684

685

686

687 *Implications for sensory processing*

688 Plasticity of TH expression is believed to be a way in which the olfactory bulb can tune its levels of
689 dopaminergic signalling according to changes in incoming sensory-evoked activity. Given some of
690 the known effects of dopamine in glomerular networks, this could potentially have the effect of
691 counteracting input activity perturbation. For example, the best-described circuit-level effect of
692 dopamine in the bulb is its inhibitory action on the release of glutamate from olfactory sensory
693 neuron axon terminals, which it achieves via D2 receptor activation (Hsia *et al.*, 1999; Berkowicz &
694 Trombley, 2000; Ennis *et al.*, 2001; Maher & Westbrook, 2008; McGann, 2013; Vaaga *et al.*, 2017). If
695 sensory input levels are chronically decreased, it might be adaptive to reduce the strength of this
696 inhibition, perhaps by decreasing expression of the rate-limiting enzyme for neurotransmitter
697 synthesis. This might put the system into a state of higher-gain readiness for the low levels of input
698 that will initially arrive if and when sensory stimulation recommences. Indeed, the volume-
699 transmission nature of sensory neuron presynaptic inhibition (Pinching & Powell, 1971; McGann,
700 2013), coupled with the high threshold and slow dynamics of bulbar dopamine release (Borisovska *et*
701 *al.*, 2013), might make for a slow modulatory process that is well suited to days-scale modification
702 via plasticity of enzyme expression. However, given the strong presynaptic inhibition also mediated
703 by $GABA_B$ receptor activation on OSN terminals (McGann, 2013), it is unclear why dopamine- but not
704 GABA-synthesising enzymes are targets for rapid activity-dependent regulation in this circuit. It may
705 be that GABAergic inhibition is modulated by distinct plastic mechanisms that do not target
706 transmitter synthesis. Alternatively, distinct mechanisms of GABAergic and dopaminergic inhibition
707 that can occur within the same presynaptic terminals (Burke *et al.*, 2018) might be individually tuned
708 according to sensory experience.

709 In contrast, the potential functional implications of TH plasticity on the less-understood postsynaptic
710 effects of bulbar dopamine transmission are harder to predict. Dopamine can act via D1-type
711 receptors to promote rebound firing after interglomerular GABAergic inhibition of external tufted
712 cells (Liu *et al.*, 2013), so perhaps decreased TH levels might lead to more prolonged lateral
713 inhibition within the glomerular layer. The implications of such an effect for information processing
714 in sensory-deprived bulbar circuits might be best addressed via computational network modelling.
715 Most important, though, is the fact that, although experience-dependent plasticity in olfactory bulb
716 TH expression has been described for decades, it is still not known how (or whether) changes in TH
717 mRNA and protein levels give rise to alterations in the amount of dopamine actually released.
718 Future experiments should be able to control the activity of dopaminergic neurons whilst monitoring
719 the resulting effects of dopamine release (e.g. Vaaga *et al.*, 2017), in order to quantitatively compare
720 the outcome in control versus sensory-deprived tissue.

721 **Acknowledgements**

722

723 This work was supported by a Medical Research Council 4-year PhD studentship to DJB, and a
724 Leverhulme Trust Research Grant (RPG-2016-095) and ERC Consolidator Grant (725729;
725 FUNCOPLAN) to MSG. We wish to thank Beatriz Rico for access to equipment, Laura Andreae and
726 Elisa Galliano for comments on the manuscript, and Elisa Galliano, Andres Crespo Vieira, Christiane
727 Hahn and other past and present members of the Grubb laboratory for technical assistance and
728 stimulating discussion.

729 **References**

730 Adam, Y. & Mizrahi, A. (2011) Long-term imaging reveals dynamic changes in the neuronal
731 composition of the glomerular layer. *J. Neurosci.*, **31**, 7967–7973.
732 Agoston, Z., Heine, P., Brill, M.S., Grebbin, B.M., Hau, A.-C., Kallenborn-Gerhardt, W., Schramm, J.,
733 Götz, M., & Schulte, D. (2014) Meis2 is a Pax6 co-factor in neurogenesis and dopaminergic
734 periglomerular fate specification in the adult olfactory bulb. *Development*, **141**, 28–38.
735 Akiba, Y., Sasaki, H., Saino-Saito, S., & Baker, H. (2007) Temporal and spatial disparity in cFOS
736 expression and dopamine phenotypic differentiation in the neonatal mouse olfactory bulb.
737 *Neurochem. Res.*, **32**, 625–634.
738 Bäckman, C.M., Malik, N., Zhang, Y., Shan, L., Grinberg, A., Hoffer, B.J., Westphal, H., & Tomac, A.C.
739 (2006) Characterization of a mouse strain expressing Cre recombinase from the 3'
740 untranslated region of the dopamine transporter locus. *Genesis*, **44**, 383–390.
741 Baker, H. (1990) Unilateral, neonatal olfactory deprivation alters tyrosine hydroxylase expression but
742 not aromatic amino acid decarboxylase or GABA immunoreactivity. *Neuroscience*, **36**, 761–
743 771.
744 Baker, H., Cummings, D.M., Munger, S.D., Margolis, J.W., Franzen, L., Reed, R.R., & Margolis, F.L.
745 (1999) Targeted deletion of a cyclic nucleotide-gated channel subunit (OCNC1): biochemical
746 and morphological consequences in adult mice. *J. Neurosci.*, **19**, 9313–9321.
747 Baker, H., Kawano, T., Albert, V., Joh, T.H., Reis, D.J., & Margolis, F.L. (1984) Olfactory bulb dopamine
748 neurons survive deafferentation-induced loss of tyrosine hydroxylase. *Neuroscience*, **11**,
749 605–615.
750 Baker, H., Kawano, T., Margolis, F.L., & Joh, T.H. (1983) Transneuronal regulation of tyrosine
751 hydroxylase expression in olfactory bulb of mouse and rat. *J. Neurosci.*, **3**, 69–78.
752 Baker, H., Morel, K., Stone, D.M., & Maruniak, J.A. (1993) Adult naris closure profoundly reduces
753 tyrosine hydroxylase expression in mouse olfactory bulb. *Brain Res.*, **614**, 109–116.
754 Banerjee, A., Marbach, F., Anselmi, F., Koh, M.S., Davis, M.B., Garcia da Silva, P., Delevich, K., Oyibo,
755 H.K., Gupta, P., Li, B., & Albeanu, D.F. (2015) An Interglomerular Circuit Gates Glomerular
756 Output and Implements Gain Control in the Mouse Olfactory Bulb. *Neuron*, **87**, 193–207.
757 Banerjee, K., Akiba, Y., Baker, H., & Cave, J.W. (2013) Epigenetic control of neurotransmitter
758 expression in olfactory bulb interneurons. *Int. J. Dev. Neurosci.*, **31**, 415–423.
759 Banerjee, K., Wang, M., Cai, E., Fujiwara, N., Baker, H., & Cave, J.W. (2014) Regulation of tyrosine
760 hydroxylase transcription by hnRNP K and DNA secondary structure. *Nat Commun*, **5**, 5769.
761 Bastien-Dionne, P.-O., David, L.S., Parent, A., & Saghatelyan, A. (2010) Role of sensory activity on
762 chemospecific populations of interneurons in the adult olfactory bulb. *J. Comp. Neurol.*, **518**,
763 1847–1861.
764 Benito, N., Gaborieau, E., Sanz Diez, A., Kosar, S., Foucault, L., Raineteau, O., & De Saint Jan, D.
765 (2018) A Pool of Postnatally Generated Interneurons Persists in an Immature Stage in the
766 Olfactory Bulb. *J. Neurosci.*, **38**, 9870–9882.
767 Berkowicz, D.A. & Trombley, P.Q. (2000) Dopaminergic modulation at the olfactory nerve synapse.
768 *Brain Res.*, **855**, 90–99.
769 Borisovska, M., Bensen, A.L., Chong, G., & Westbrook, G.L. (2013) Distinct modes of dopamine and
770 GABA release in a dual transmitter neuron. *J. Neurosci.*, **33**, 1790–1796.
771 Brill, M.S., Snapyan, M., Wohlfrom, H., Ninkovic, J., Jawerka, M., Mastick, G.S., Ashery-Padan, R.,
772 Saghatelyan, A., Berninger, B., & Götz, M. (2008) A dlx2- and pax6-dependent transcriptional
773 code for periglomerular neuron specification in the adult olfactory bulb. *J. Neurosci.*, **28**,
774 6439–6452.
775 Burke, K.J., Keeshen, C.M., & Bender, K.J. (2018) Two Forms of Synaptic Depression Produced by
776 Differential Neuromodulation of Presynaptic Calcium Channels. *Neuron*, **99**, 969-984.e7.
777 Bustin, S.A., Benes, V., Garson, J.A., Hellemans, J., Huggett, J., Kubista, M., Mueller, R., Nolan, T.,
778 Pfaffl, M.W., Shipley, G.L., Vandesompele, J., & Wittwer, C.T. (2009) The MIQE guidelines:

779 minimum information for publication of quantitative real-time PCR experiments. *Clin. Chem.*,
780 **55**, 611–622.
781 Bywalez, W.G., Ona-Jodar, T., Lukas, M., Ninkovic, J., & Egger, V. (2016) Dendritic Arborization
782 Patterns of Small Juxtaglomerular Cell Subtypes within the Rodent Olfactory Bulb. *Front*
783 *Neuroanat*, **10**, 127.
784 Cave, J.W., Akiba, Y., Banerjee, K., Bhosle, S., Berlin, R., & Baker, H. (2010) Differential regulation of
785 dopaminergic gene expression by Er81. *J. Neurosci.*, **30**, 4717–4724.
786 Chand, A.N., Galliano, E., Chesters, R.A., & Grubb, M.S. (2015) A distinct subtype of dopaminergic
787 interneuron displays inverted structural plasticity at the axon initial segment. *J. Neurosci.*,
788 **35**, 1573–1590.
789 Cheetham, C.E.J., Park, U., & Belluscio, L. (2016) Rapid and continuous activity-dependent plasticity
790 of olfactory sensory input. *Nat Commun*, **7**, 10729.
791 Cho, J.Y., Min, N., Franzen, L., & Baker, H. (1996) Rapid down-regulation of tyrosine hydroxylase
792 expression in the olfactory bulb of naris-occluded adult rats. *J. Comp. Neurol.*, **369**, 264–276.
793 Cigola, E., Volpe, B.T., Lee, J.W., Franzen, L., & Baker, H. (1998) Tyrosine hydroxylase expression in
794 primary cultures of olfactory bulb: role of L-type calcium channels. *J. Neurosci.*, **18**, 7638–
795 7649.
796 Cockerham, R., Liu, S., Cachope, R., Kiyokage, E., Cheer, J.F., Shipley, M.T., & Puche, A.C. (2016)
797 Subsecond Regulation of Synaptically Released Dopamine by COMT in the Olfactory Bulb. *J.*
798 *Neurosci.*, **36**, 7779–7785.
799 Coppola, D.M. (2012) Studies of olfactory system neural plasticity: the contribution of the unilateral
800 naris occlusion technique. *Neural Plast.*, **2012**, 351752.
801 Cummings, D.M., Henning, H.E., & Brunjes, P.C. (1997) Olfactory bulb recovery after early sensory
802 deprivation. *J. Neurosci.*, **17**, 7433–7440.
803 Ennis, M., Zhou, F.M., Ciombor, K.J., Aroniadou-Anderjaska, V., Hayar, A., Borrelli, E., Zimmer, L.A.,
804 Margolis, F., & Shipley, M.T. (2001) Dopamine D2 receptor-mediated presynaptic inhibition
805 of olfactory nerve terminals. *J. Neurophysiol.*, **86**, 2986–2997.
806 Fogli Iseppe, A., Pignatelli, A., & Belluzzi, O. (2016) Calretinin-Periglomerular Interneurons in Mice
807 Olfactory Bulb: Cells of Few Words. *Front Cell Neurosci*, **10**, 231.
808 Fokkens, W.J., Lund, V.J., Mullol, J., Bachert, C., Alobid, I., Baroody, F., Cohen, N., Cervin, A., Douglas,
809 R., Gevaert, P., Georgalas, C., Goossens, H., Harvey, R., Hellings, P., Hopkins, C., Jones, N.,
810 Joos, G., Kalogjera, L., Kern, B., Kowalski, M., Price, D., Riechelmann, H., Schlosser, R., Senior,
811 B., Thomas, M., Toskala, E., Voegels, R., Wang, D.Y., & Wormald, P.J. (2012) EPOS 2012:
812 European position paper on rhinosinusitis and nasal polyps 2012. A summary for
813 otorhinolaryngologists. *Rhinology*, **50**, 1–12.
814 Galliano, E., Franzoni, E., Breton, M., Chand, A.N., Byrne, D.J., Murthy, V.N., & Grubb, M.S. (2018)
815 Embryonic and postnatal neurogenesis produce functionally distinct subclasses of
816 dopaminergic neuron. *Elife*, **7**.
817 Galliano, E., Hahn, C., Browne, L., Villamayor, P.R., & Grubb, M.S. (2020) Brief sensory deprivation
818 triggers cell type-specific structural and functional plasticity in olfactory bulb neurons.
819 *bioRxiv*, 2020.05.10.086926.
820 Grier, B.D., Belluscio, L., & Cheetham, C.E.J. (2016) Olfactory Sensory Activity Modulates Microglial-
821 Neuronal Interactions during Dopaminergic Cell Loss in the Olfactory Bulb. *Front Cell*
822 *Neurosci*, **10**, 178.
823 Hadjiconstantinou, M., Wemlinger, T.A., Sylvia, C.P., Hubble, J.P., & Neff, N.H. (1993) Aromatic L-
824 amino acid decarboxylase activity of mouse striatum is modulated via dopamine receptors. *J.*
825 *Neurochem.*, **60**, 2175–2180.
826 Halász, N., Ljungdahl, A., Hökfelt, T., Johansson, O., Goldstein, M., Park, D., & Biberfeld, P. (1977)
827 Transmitter histochemistry of the rat olfactory bulb. I. Immunohistochemical localization of
828 monoamine synthesizing enzymes. Support for intrabulbar, periglomerular dopamine
829 neurons. *Brain Res.*, **126**, 455–474.

830 Hayar, A., Karnup, S., Shipley, M.T., & Ennis, M. (2004) Olfactory Bulb Glomeruli: External Tufted
831 Cells Intrinsically Burst at Theta Frequency and Are Entrained by Patterned Olfactory Input. *J.*
832 *Neurosci.*, **24**, 1190–1199.
833 Heffner, C.S., Herbert Pratt, C., Babiuk, R.P., Sharma, Y., Rockwood, S.F., Donahue, L.R., Eppig, J.T., &
834 Murray, S.A. (2012) Supporting conditional mouse mutagenesis with a comprehensive cre
835 characterization resource. *Nat Commun*, **3**, 1218.
836 Hökfelt, T., Halasz, N., Ljungdahl, A., Johansson, O., Goldstein, M., & Park, D. (1975) Histochemical
837 support for a dopaminergic mechanism in the dendrites of certain periglomerular cells in the
838 rat olfactory bulb. *Neurosci. Lett.*, **1**, 85–90.
839 Hsia, A.Y., Vincent, J.D., & Lledo, P.M. (1999) Dopamine depresses synaptic inputs into the olfactory
840 bulb. *J. Neurophysiol.*, **82**, 1082–1085.
841 Kass, M.D., Pottackal, J., Turkel, D.J., & McGann, J.P. (2013) Changes in the neural representation of
842 odorants after olfactory deprivation in the adult mouse olfactory bulb. *Chem. Senses*, **38**,
843 77–89.
844 Kikuta, S., Sakamoto, T., Nagayama, S., Kanaya, K., Kinoshita, M., Kondo, K., Tsunoda, K., Mori, K., &
845 Yamasoba, T. (2015) Sensory deprivation disrupts homeostatic regeneration of newly
846 generated olfactory sensory neurons after injury in adult mice. *J. Neurosci.*, **35**, 2657–2673.
847 Kiyokage, E., Pan, Y.-Z., Shao, Z., Kobayashi, K., Szabo, G., Yanagawa, Y., Obata, K., Okano, H., Toida,
848 K., Puche, A.C., & Shipley, M.T. (2010) Molecular identity of periglomerular and short axon
849 cells. *J. Neurosci.*, **30**, 1185–1196.
850 Kohwi, M., Petryniak, M.A., Long, J.E., Ekker, M., Obata, K., Yanagawa, Y., Rubenstein, J.L.R., &
851 Alvarez-Buylla, A. (2007) A subpopulation of olfactory bulb GABAergic interneurons is
852 derived from Emx1- and Dlx5/6-expressing progenitors. *J. Neurosci.*, **27**, 6878–6891.
853 Kosaka, K. & Kosaka, T. (2007) Chemical properties of type 1 and type 2 periglomerular cells in the
854 mouse olfactory bulb are different from those in the rat olfactory bulb. *Brain Res.*, **1167**, 42–
855 55.
856 Kosaka, T. & Kosaka, K. (2011) “Interneurons” in the olfactory bulb revisited. *Neurosci. Res.*, **69**, 93–
857 99.
858 Kosaka, T., Kosaka, K., Hama, K., Wu, J.Y., & Nagatsu, I. (1987) Differential effect of functional
859 olfactory deprivation on the GABAergic and catecholaminergic traits in the rat main olfactory
860 bulb. *Brain Res.*, **413**, 197–203.
861 Kosaka, T., Pignatelli, A., & Kosaka, K. (2019) Heterogeneity of tyrosine hydroxylase expressing
862 neurons in the main olfactory bulb of the mouse. *Neurosci. Res.*,.
863 Lammel, S., Steinberg, E.E., Földy, C., Wall, N.R., Beier, K., Luo, L., & Malenka, R.C. (2015) Diversity of
864 transgenic mouse models for selective targeting of midbrain dopamine neurons. *Neuron*, **85**,
865 429–438.
866 Lau, C.G. & Murthy, V.N. (2012) Activity-dependent regulation of inhibition via GAD67. *J. Neurosci.*,
867 **32**, 8521–8531.
868 Liu, N., Cigola, E., Tinti, C., Jin, B.K., Conti, B., Volpe, B.T., & Baker, H. (1999) Unique regulation of
869 immediate early gene and tyrosine hydroxylase expression in the odor-deprived mouse
870 olfactory bulb. *J. Biol. Chem.*, **274**, 3042–3047.
871 Liu, S., Plachez, C., Shao, Z., Puche, A., & Shipley, M.T. (2013) Olfactory bulb short axon cell release of
872 GABA and dopamine produces a temporally biphasic inhibition-excitation response in
873 external tufted cells. *J. Neurosci.*, **33**, 2916–2926.
874 Liu, S., Puche, A.C., & Shipley, M.T. (2016) The Interglomerular Circuit Potently Inhibits Olfactory
875 Bulb Output Neurons by Both Direct and Indirect Pathways. *J. Neurosci.*, **36**, 9604–9617.
876 Livak, K.J. & Schmittgen, T.D. (2001) Analysis of Relative Gene Expression Data Using Real-Time
877 Quantitative PCR and the 2−ΔΔCT Method. *Methods*, **25**, 402–408.
878 Maher, B.J. & Westbrook, G.L. (2008) Co-transmission of dopamine and GABA in periglomerular
879 cells. *J. Neurophysiol.*, **99**, 1559–1564.

880 Mandairon, N., Sacquet, J., Jourdan, F., & Didier, A. (2006) Long-term fate and distribution of
881 newborn cells in the adult mouse olfactory bulb: Influences of olfactory deprivation.
882 *Neuroscience*, **141**, 443–451.
883 McGann, J.P. (2013) Presynaptic inhibition of olfactory sensory neurons: new mechanisms and
884 potential functions. *Chem. Senses*, **38**, 459–474.
885 Nadi, N.S., Head, R., Grillo, M., Hempstead, J., Grannot-Reisfeld, N., & Margolis, F.L. (1981) Chemical
886 deafferentation of the olfactory bulb: plasticity of the levels of tyrosine hydroxylase,
887 dopamine and norepinephrine. *Brain Res.*, **213**, 365–377.
888 Ninkovic, J., Pinto, L., Petricca, S., Lepier, A., Sun, J., Rieger, M.A., Schroeder, T., Cvekl, A., Favor, J., &
889 Götz, M. (2010) The transcription factor Pax6 regulates survival of dopaminergic olfactory
890 bulb neurons via crystallin αA. *Neuron*, **68**, 682–694.
891 Panzanelli, P., Fritschy, J.M., Yanagawa, Y., Obata, K., & Sassoè-Pognetto, M. (2007) GABAergic
892 phenotype of periglomerular cells in the rodent olfactory bulb. *Journal of Comparative*
893 *Neurology*, **502**, 990–1002.
894 Parrish-Aungst, S., Kiyokage, E., Szabo, G., Yanagawa, Y., Shipley, M.T., & Puche, A.C. (2011) Sensory
895 experience selectively regulates transmitter synthesis enzymes in interglomerular circuits.
896 *Brain Res.*, **1382**, 70–76.
897 Parrish-Aungst, S., Shipley, M.T., Erdelyi, F., Szabo, G., & Puche, A.C. (2007) Quantitative analysis of
898 neuronal diversity in the mouse olfactory bulb. *J. Comp. Neurol.*, **501**, 825–836.
899 Philpot, B.D., Men, D., McCarty, R., & Brunjes, P.C. (1998) Activity-dependent regulation of
900 dopamine content in the olfactory bulbs of naris-occluded rats. *Neuroscience*, **85**, 969–977.
901 Pignatelli, A., Ackman, J.B., Vigetti, D., Beltrami, A.P., Zucchini, S., & Belluzzi, O. (2009) A potential
902 reservoir of immature dopaminergic replacement neurons in the adult mammalian olfactory
903 bulb. *Pflugers Arch.*, **457**, 899–915.
904 Pignatelli, A. & Belluzzi, O. (2017) Dopaminergic Neurones in the Main Olfactory Bulb: An Overview
905 from an Electrophysiological Perspective. *Front Neuroanat*, **11**, 7.
906 Pignatelli, A., Kobayashi, K., Okano, H., & Belluzzi, O. (2005) Functional properties of dopaminergic
907 neurones in the mouse olfactory bulb. *J. Physiol. (Lond.)*, **564**, 501–514.
908 Pinching, A.J. & Powell, T.P. (1971) The neuropil of the periglomerular region of the olfactory bulb. *J.*
909 *Cell. Sci.*, **9**, 379–409.
910 Rosser, A.E., Hökfelt, T., & Goldstein, M. (1986) LHRH and catecholamine neuronal systems in the
911 olfactory bulb of the mouse. *Journal of Comparative Neurology*, **250**, 352–363.
912 Saino-Saito, S., Sasaki, H., Volpe, B.T., Kobayashi, K., Berlin, R., & Baker, H. (2004) Differentiation of
913 the dopaminergic phenotype in the olfactory system of neonatal and adult mice. *J. Comp.*
914 *Neurol.*, **479**, 389–398.
915 Sato, T., Homma, R., & Nagayama, S. (2020) Direct comparison of odor responses of homologous
916 glomeruli in the medial and lateral maps of the mouse olfactory bulb. *eNeuro*,.
917 Short, S.M. & Wachowiak, M. (2019) Temporal Dynamics of Inhalation-Linked Activity across Defined
918 Subpopulations of Mouse Olfactory Bulb Neurons Imaged In Vivo. *eNeuro*, **6**.
919 Stone, D.M., Grillo, M., Margolis, F.L., Joh, T.H., & Baker, H. (1991) Differential effect of functional
920 olfactory bulb deafferentation on tyrosine hydroxylase and glutamic acid decarboxylase
921 messenger RNA levels in rodent juxtaglomerular neurons. *J. Comp. Neurol.*, **311**, 223–233.
922 Stone, D.M., Wessel, T., Joh, T.H., & Baker, H. (1990) Decrease in tyrosine hydroxylase, but not
923 aromatic L-amino acid decarboxylase, messenger RNA in rat olfactory bulb following
924 neonatal, unilateral odor deprivation. *Brain Res. Mol. Brain Res.*, **8**, 291–300.
925 Tavakoli, A., Schmaltz, A., Schwarz, D., Margrie, T.W., Schaefer, A.T., & Kollo, M. (2018) Quantitative
926 Association of Anatomical and Functional Classes of Olfactory Bulb Neurons. *J. Neurosci.*, **38**,
927 7204–7220.
928 Taylor, S.C., Nadeau, K., Abbasi, M., Lachance, C., Nguyen, M., & Fenrich, J. (2019) The Ultimate qPCR
929 Experiment: Producing Publication Quality, Reproducible Data the First Time. *Trends in*
930 *Biotechnology*, **37**, 761–774.

931 Vaaga, C.E., Yorgason, J.T., Williams, J.T., & Westbrook, G.L. (2017) Presynaptic gain control by
932 endogenous cotransmission of dopamine and GABA in the olfactory bulb. *J. Neurophysiol.*,
933 **117**, 1163–1170.
934 Vlug, A.S., Teuling, E., Haasdijk, E.D., French, P., Hoogenraad, C.C., & Jaarsma, D. (2005) ATF3
935 expression precedes death of spinal motoneurons in amyotrophic lateral sclerosis-SOD1
936 transgenic mice and correlates with c-Jun phosphorylation, CHOP expression, somato-
937 dendritic ubiquitination and Golgi fragmentation. *Eur. J. Neurosci.*, **22**, 1881–1894.
938 Wachowiak, M., Economo, M.N., Díaz-Quesada, M., Brunert, D., Wesson, D.W., White, J.A., &
939 Rothermel, M. (2013) Optical dissection of odor information processing in vivo using
940 GCaMPs expressed in specified cell types of the olfactory bulb. *J. Neurosci.*, **33**, 5285–5300.
941 Wang, M., Cai, E., Fujiwara, N., Fones, L., Brown, E., Yanagawa, Y., & Cave, J.W. (2017) Odorant
942 Sensory Input Modulates DNA Secondary Structure Formation and Heterogeneous
943 Ribonucleoprotein Recruitment on the Tyrosine Hydroxylase and Glutamic Acid
944 Decarboxylase 1 Promoters in the Olfactory Bulb. *J. Neurosci.*, **37**, 4778–4789.
945 Weiss, J., Pyrski, M., Jacobi, E., Bufe, B., Willnecker, V., Schick, B., Zizzari, P., Gossage, S.J., Greer,
946 C.A., Leinders-Zufall, T., Woods, C.G., Wood, J.N., & Zufall, F. (2011) Loss-of-function
947 mutations in sodium channel Nav1.7 cause anosmia. *Nature*, **472**, 186–190.
948 Wilson, D.A. & Sullivan, R.M. (1995) The D2 antagonist spiperone mimics the effects of olfactory
949 deprivation on mitral/tufted cell odor response patterns. *J. Neurosci.*, **15**, 5574–5581.
950 Zeisel, A., Hochgerner, H., Lönnerberg, P., Johnsson, A., Memic, F., van der Zwan, J., Häring, M.,
951 Braun, E., Borm, L.E., La Manno, G., Codeluppi, S., Furlan, A., Lee, K., Skene, N., Harris, K.D.,
952 Hjerling-Leffler, J., Arenas, E., Ernfors, P., Marklund, U., & Linnarsson, S. (2018) Molecular
953 Architecture of the Mouse Nervous System. *Cell*, **174**, 999-1014.e22.
954 Zhu, M.Y., Juorio, A.V., Paterson, I.A., & Boulton, A.A. (1993) Regulation of striatal aromatic L-amino
955 acid decarboxylase: effects of blockade or activation of dopamine receptors. *Eur. J.*
956 *Pharmacol.*, **238**, 157–164.
957